CSIRO PUBLISHING

SPECIAL ISSUE | ACCOUNT
https://doi.org/10.1071/CH22205

AUSTRALIAN JOURNAL OF CHEMISTRY

Mutagenicity of *N*-acyloxy-*N*-alkoxyamides – QSAR determination of factors controlling activity

Stephen A. Glover[A,*]

For full list of author affiliations and declarations see end of paper

***Correspondence to:**
Stephen A. Glover
Department of Chemistry, School of Physical Sciences, University of New England, NSW 2350, Australia
Email: sglover@une.edu.au

Handling Editor:
Curt Wentrup

ABSTRACT

This account describes the origins of our extensive investigations into the mutagenicity of *N*-acyloxy-*N*-alkoxyamides. Since their discovery as biologically active anomeric amides that mutate DNA in the Ames reverse mutation assay without the need for metabolic activation, we have used activities in the Ames test to understand the impact of structural variation on cellular access to, binding to and reactivity with DNA. We have developed an understanding of the roles played by hydrophobicity, electrophilic reactivity, steric effects and, importantly, intercalation on mutagenicity levels and therefore interactions with DNA. The evolution and application of meaningful quantitative structure–activity relationships is described, and examples of their utility in explaining molecule–DNA interactions are given. Their ability to explain previous mutagenicity data and, importantly, to predict meaningful mutagenic behaviour is also demonstrated.

Keywords: acyloxy alkoxyamides, ames mutagenicity, anomeric amides, bilinear QSAR, deamination, direct-acting mutagenicity, DNA binding, groove binding, HERON reactions, intercalation, linear QSAR, mutagenic amides, nitrogen deletion, PAH, pyramidal amides, QSAR, quantitative structure–activity relationship, skeletal editing, TA98, TA100.

Introduction

N-Acyloxy-*N*-alkoxyamides (NAAs), **2**, are members of the unusual class of anomeric amides **1**, which we defined as amides bearing two electronegative heteroatoms bonded to the amide nitrogen (Chart 1).[1] These have unusual properties. Firstly, through Bent's Rule,[2,3] the electron demand of the electronegative substituents in **1** imparts more p character to the nitrogen hybrid orbitals bonded to them, with a concomitant increase in s character in the nitrogen lone pair orbital. Hence, these amides possess distinctly pyramidal nitrogens.[1,4–13] This, combined with the lower-energy lone pair, results in diminished amide resonance. Secondly, anomeric interactions between the nitrogen substituents results in unusual chemistry at the amide nitrogen.

In the case of *N*-acyloxy-*N*-alkoxyamides **2**, the nitrogen is bonded to two oxygen atoms and, as a result, they are strongly pyramidal at nitrogen, evidence for which stems from X-ray structures[7] as well as computational data.[8,9,13] Several NAAs we have made are the most pyramidal amides known.[7] The combined electronegativity results in a very significant reduction in resonance, estimated computationally to be ~50% that of the iconic standard amide *N*,*N*-dimethylacetamide, and manifests itself in longer amide bonds.[7,8,13] These structural properties are borne out spectroscopically, most notably by infrared spectroscopy where the amide carbonyl stretch frequencies are considerably higher than found in primary, secondary and tertiary amides. Typically, these are in the range of 1718–1742 cm^{-1} on average, some 50–54 cm^{-1} higher than their precursor hydroxamic esters.[8]

Although two anomeric interactions are possible in NAAs (Fig. 1), because the acyloxyl group would be more electron-demanding, the more favourable anomeric interaction at the amide nitrogen involves donation of the alkoxyl oxygen lone pair into the σ* orbital between nitrogen and the acyloxyl oxygen (n_{OR}–σ^*_{NOAcyl}) for which there is structural and theoretical evidence.[7,8,13] The destabilisation of the bond to the acyloxyl group renders NAAs susceptible to both unimolecular and bimolecular reactions

Received: 23 September 2022
Accepted: 27 October 2022
Published: 19 January 2023

Cite this:
Glover SA (2023)
Australian Journal of Chemistry
76(1), 1–24. doi:10.1071/CH22205

at nitrogen. Under conditions of acid catalysis, they react by the unusual $A_{Al}1$ mechanism, producing nitrenium ion intermediates.[14,15] However, they undergo S_N2 reactions at nitrogen with a range of nucleophiles including amines (path i, Scheme 1),[16–20] azides (path ii, Scheme 1),[21] hydroxides (path iii, Scheme 1)[22] and thiols (path iv, Scheme 1),[23] each process producing new anomeric amide intermediates that react further. All these processes occur at ambient temperatures. At higher temperatures, NAAs undergo the novel HERON reaction, producing anhydrides and alkoxynitrenes in competition with homolysis (path vi and vii, Scheme 1).[24]

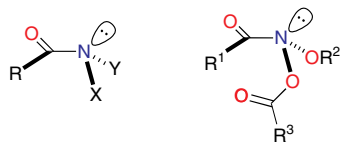

1 **2**

a: X = Cl, Y = OR
b: X = OAc, Y = OR
c: X = Y = OR
d: X = OR, Y = NR_2
e: X = OR, Y = SR

Chart 1. 1. Anomeric amides, 2. *N*-acyloxy-*N*-alkoxyamides (NAAs).

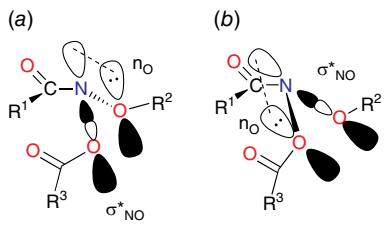

Fig. 1. Two possible anomeric interactions in anomeric amides: (*a*) n_{OR}–σ^*_{NOAcyl}, and (*b*) n_{OAcyl}–σ^*_{NOR}.

We originally investigated the chemical properties of NAAs as *N*-alkoxyl analogues of *N*-acetoxy-*N*-arylacetamides **4**, one penultimate carcinogenic metabolite of aromatic amines **3** such as carcinogenic 2-acetylaminofluorene or 4-acetylaminobiphenyl (Scheme 2).[25–29] These produce by solvolysis *N*-acetyl-*N*-arylnitrenium ions **7**, the ultimate electrophilic carcinogenic metabolites, which react with DNA.[30–33]

In foundation chemistry, we synthesised *N*-acetoxy-*N*-alkoxymides **5** for the first time from hydroxamic esters **6** by chlorination at nitrogen followed by reaction with silver acetate and found them to be mutagenic in the Ames test.[14,34,35] *N*-acyl-*N*-alkoxynitrenium ions **8** and *N*-acetyl-*N*-arylnitrenium ions **7** are similarly resonance-stabilised,[36,37] so by analogy with **4**, we envisaged that **5** could undergo solvolysis to **8**, which could react with nucleophilic centres in DNA (Scheme 2, dashed route). However, *in vitro* DNA damage studies demonstrated that NAAs bind and react intact with plasmid DNA primarily at G-N7 in the major groove and, to a lesser degree, at A-N3 in the minor groove (Scheme 2, solid arrow; path v, Scheme 1), rather than through the intermediacy of nitrenium ions **8**.[38,39] Furthermore, both the acyloxyl and an alkoxyl substituent at nitrogen are determinants of reactivity with DNA.[38] Not surprisingly therefore, NAAs are direct-acting mutagens reverting the point mutation strain *Salmonella typhimurium* TA100 to wild type in the Ames reverse mutation assay *without* the need for metabolic activation.[34,40] Reactions with *N*-methylaniline have been widely studied kinetically to determine factors affecting S_N2 reactivity, as this was deemed pivotal in their behaviour within the major groove of DNA.[16,18–20]

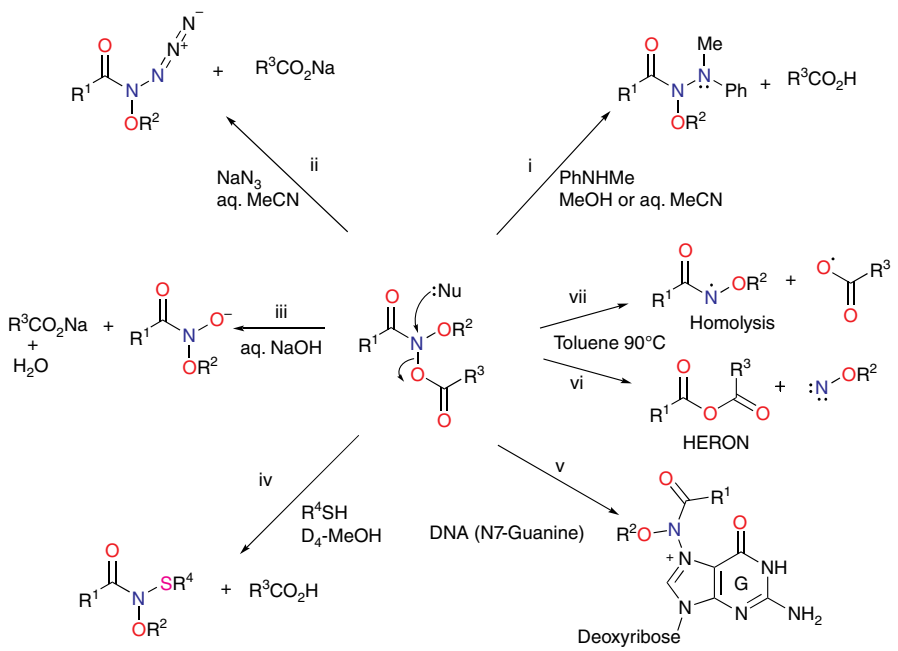

Scheme 1. Reactions of *N*-acyloxy-*N*-alkoxyamides.

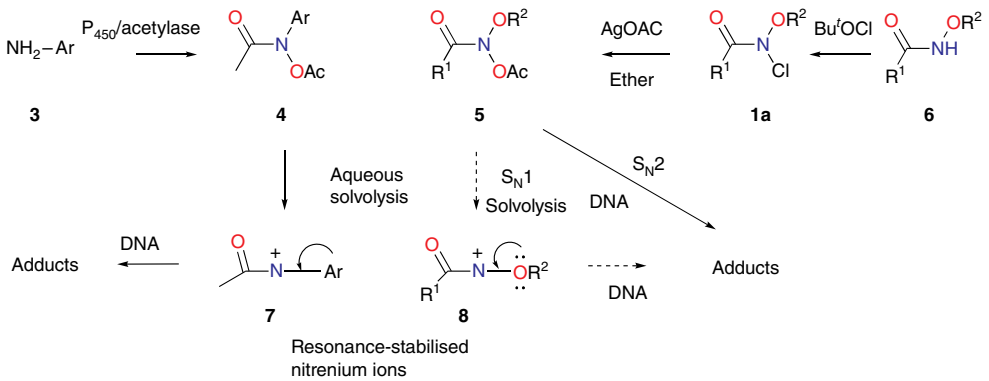

Scheme 2. Parallels between aromatic amine metabolites *N*-acetoxy-*N*-arylacetamides **4** and *N*-acyloxy-*N*-alkoxyamides **5**.

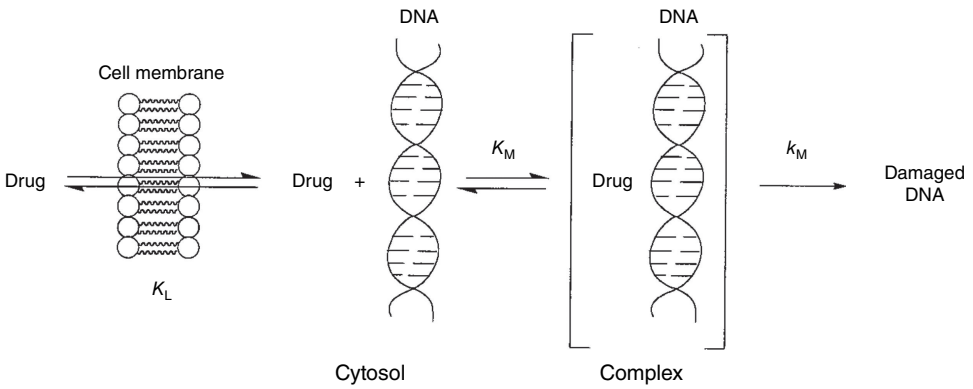

Fig. 2. Elemental processes in the reaction of *N*-acyloxy-*N*-alkoxyamides with DNA. Reproduced from Ref. [42] with permission from the Royal Society of Chemistry.

In the full-plate incorporation assay used throughout our Ames investigations, point mutations result in countable colonies,[41] and at the outset, we found that in nearly all cases the NAAs gave a linear dose response, the gradient of which afforded LogTA100, the $\log_{10}$ of induced revertants at 1 μmol per plate.[40] A comparison of activities at 1 μmol per plate enabled us to investigate factors that both promoted and inhibited their mutagenic activity. In all, we have determined comparative data for some 100 NAAs.

The Ames methodology involves some variability in testing medium and therefore background reversion rates. However, to counteract this, we tested every new compound in parallel with a single compound, *N*-butoxy-*N*-acetoxybenzamide (**9**, X = H). In this manner, all new data could be scaled to the activity of this standard. As a consequence, changes in LogTA100 could be sheeted home to alterations in structure rather than assay variability. This proved to be pivotal in determining structural influence on a range of cellular and intracellular processes. As the target giving rise to reverse mutation in bacterial TA100 must be cytosolic DNA, we have been able to use standardised Ames mutagenicity to deduce factors affecting the transport to, binding with and reactions with DNA from correlations between chemical structure and activity.

Fig. 2 illustrates the various intervening processes involved in the ultimate damage to DNA. Passage through the cell wall and associated equilibrium constant, K_L, is governed by lipophilicity and is a function of log*P*, $\log_{10}$ of the octanol/water partition coefficient for the molecule. Reaction with cytosolic DNA must depend on binding in the major (G-N7) and minor (A-N3) grooves and be governed by binding constant K_M, which must also depend, in part, on log*P*. However, K_M must also be related to other factors such as steric bulk or the dimensions of the mutagen, or structural aspects that enhance binding to DNA such as intercalation. The final determinant of DNA damage is the rate constant for bimolecular reaction with the nucleophilic centres in DNA, k_M, which can be dictated by factors affecting the electrophilicity of the amide nitrogen and conformation for S_N2 attack at the amide nitrogen. In the course of our studies, we have encountered structural elements impacting on all of these processes.

A review of the mutagenicity of NAAs covering early correlations appeared in 2008 as part of a wider study of the structure, reactivity and biological activity of NAAs and led to the first working quantitative structure–activity relationship (QSAR).[8] This account serves to build on this and to demonstrate applications of higher-level QSARs to gain insights into transport, DNA binding and reactivity of NAAs with DNA.

Development of a linear QSAR

As with most drug interactions, the hydrophobicity of NAAs is a critical determinant of activity.[43–48] In this host–guest relationship, hydrophobicity is important for binding in the hydrophobic grooves of DNA. Hence, log*P* is an important molecular property. Throughout our studies on NAAs, we have computed this according to the Ghose–Crippen model,[49] values for which are readily determined in most computational chemistry packages.

The importance of steric effects will be discussed at a later point, but initial mutagenicity data from series of mutagens bearing *para*-substituted phenyl groups on all three side chains (**9–11**, Chart 2) indicated that, whereas log*P* for *para*-*tert*-butylphenyl-substituted systems (X, Y and Z = Bu^t) was much larger than for *para*-methylphenyl-substituted systems (X, Y and Z = Me), activities as determined by LogTA100 were lower in each case. Similarly, *para*-phenyl groups (X, Y and Z = Ph) with much larger log*P* afforded only modest increases in LogTA100.[50] In development of QSARs, Taft steric parameters for *para*-phenyl substituents were deemed to be representative of these steric effects and, where relevant, were incorporated as E_s^1, E_s^2 and E_s^3 for *para* substituents on benzamide, benzyloxy and benzoyloxy phenyl rings respectively.[43,51]

Reactivity at the amide nitrogen was seen to be a significant determinant of activity. As substituents on a benzamide or benzyloxyl sidechains are fairly remote from the reactive nitrogen, they were not expected to impact measurably on activity. In the case of a series of *para*-substituted *N*-acetoxy-*N*-butoxybenzamides **9**, this was borne out by relative rates of S_N2 reactivity with *N*-methylaniline, which correlated very weakly with Hammett σ constants (reaction constant $\rho = 0.13$).[18,19] The electronic effect of *para*-substituents on a benzoyloxyl group in *N*-alkoxy-*N*-benzoyloxyamides was very different. Bimolecular rate constants for the reaction of *N*-methylaniline with a series of *N*-benzyloxy-*N*-(*para*-substituted-benzoyloxy)benzamides **11** correlated strongly with Hammett σ constants ($\rho = 1.69$)[18,19] in support of the modelled charge-separated S_N2 transition state, which invokes partial negative and positive charge on the leaving group and nucleophilic nitrogen respectively.[8,16,17,19] In addition, we demonstrated that rates constants for S_N2 reaction of a range of *N*-alkanoyloxyl and benzoyloxyl amides with *N*-methylaniline, k^{303}, correlate negatively with pK_a of the departing carboxylic acid group (Eqn 1).[16] However, mutagenicity of a series of *N*-benzyloxy-*N*-(*para*-substituted-benzoyloxy)benzamides correlated negatively with Hammett σ constants ($\rho = -0.57$)[22] or positively with the pK_a of the carboxylic acid (Eqn 2); the more reactive an NAA, the greater the probability that it will react with adventitious intracellular nucleophiles prior to binding to DNA, thereby lowering the effective concentration.

$$\ln k^{303} = -4.7(\pm 0.3)\mathrm{p}K_a + 18(\pm 1), \quad r = 0.986 \quad (1)$$

$$\mathrm{LogTA100} = 0.39\,\mathrm{p}K_a + 1.5, \quad r = 0.8 \quad (2)$$

Several earlier QSARs based on limited data[8,50] culminated in a QSAR based on log*P*, pK_a of the leaving group and Taft E_s^1, E_s^2 and E_s^3, which performed well for 50 analogues (Eqn 3, Fig. 3, open squares).[52] correlation coefficient, *r*, standard error, *s*, *F-statistic* and the leave-

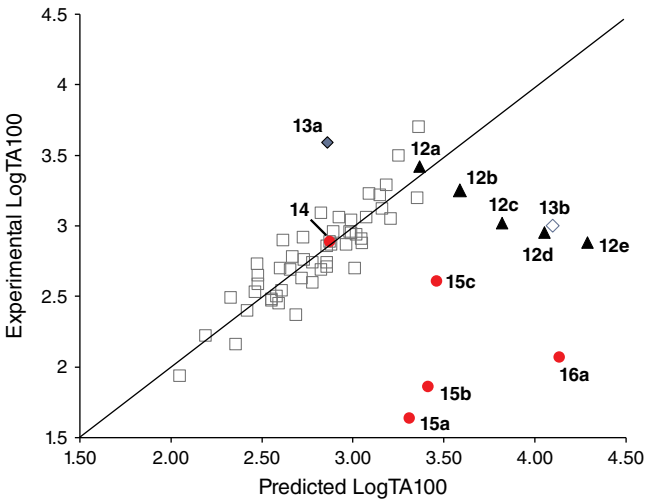

Fig. 3. Predicted vs experimental mutagenicities as LogTA100 for 50 members of the training set (open squares), **12a–e** (filled triangles), **13a** (filled diamond), **13b** (open diamond) and **14**, **15a–c**, **16a** (closed circles) in *Salmonella typhimurium* TA100 using the linear QSAR in Eqn 3.

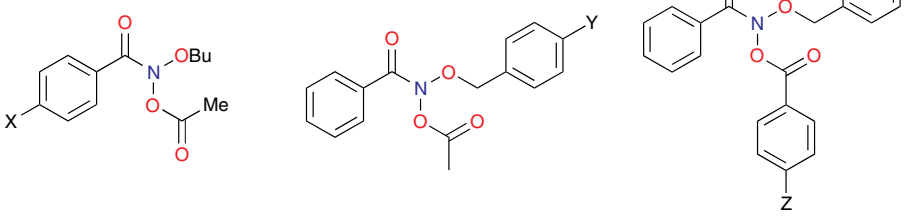

9 **10** **11**

Chart 2. NAAs bearing *para*-substituted phenyl groups.

one-out cross validation index, Q^2, all point to reasonable predictive ability.

$$\begin{aligned}\text{LogTA100} &= 1.02\,(\pm 0.41) + 0.28(\pm 0.03)\log P \\ &+ 0.18\,(\pm 0.08)\text{p}K_\text{a} + 0.13\,(\pm 0.03)E_s{}^1 \\ &+ 0.15\,(\pm 0.04)E_s{}^2 + 0.11\,(\pm 0.05)E_s{}^3 \end{aligned} \quad (3)$$

$n = 50$, $r = 0.89$, $s = 0.16$, $F = 34$, LOOCV $Q^2 = 0.70$.

Hydrophobicity and development of a bilinear QSAR

At the time of publication of such relationships, it was deemed unusual for direct-acting mutagens to show a log*P* dependence because binding to activating enzymes in metabolism was not important.[43,45,53] Where mutagens or other molecules require metabolic activation, the role of structural change and log*P* becomes less clear owing to its effect on binding to enzymes, which may be the determining factor. The modest dependence on log*P* is clear cut in the case of these direct-acting mutagens and relates to binding to DNA. These molecules are small and the bacterial strains developed by Ames are altered by the *rfa* mutation, rendering their cell walls more permeable to bulky molecules.[41,54] Drug-like compounds are more than likely to have a log*P* < 5 and, similarly, direct-acting mutagens acting on *Salmonella typhimurium* would be expected to conform to this rule.[55] However, in a series of NAAs bearing long aliphatic chains **12** (Chart 3), a significant deviation from the predicted LogTA100 was observed.[52] Moreover, the deviation was log*P*-dependent (Fig. 3, solid triangles, Table 1). Whereas the activity of **12a** was well predicted by the QSAR in Eqn 3, activities of **12b–e** deviated progressively from their predicted values with increasing log*P*. Though unrelated to the benzamides, the deviation from the predicted activity for the naphthamide **13b** bearing long aliphatic chains on the alkoxyl and acyloxyl group was also significant (Fig. 3, open diamond).

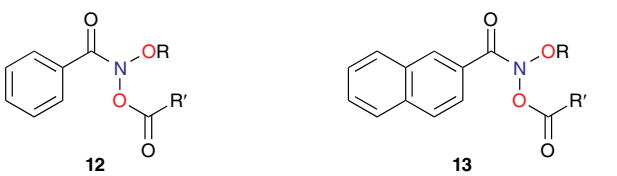

12

a R = $(CH_2)_5CH_3$, R′ = $(CH_2)_4CH_3$
b R = $(CH_2)_6CH_3$, R′ = $(CH_2)_5CH_3$
c R = $(CH_2)_7CH_3$, R′ = $(CH_2)_6CH_3$
d R = $(CH_2)_8CH_3$, R′ = $(CH_2)_7CH_3$
e R = $(CH_2)_9CH_3$, R′ = $(CH_2)_8CH_3$

13

a R = $(CH_2)_3CH_3$, R′ = CH_3
b R = $(CH_2)_7CH_3$, R′ = $(CH_2)_6CH_3$

Chart 3. NAAs bearing long, hydrophobic aliphatic chains.

The decrease in mutagenicity relative to their predicted activity can be ascribed to lipid entrapment through membrane localisation and a reduced K_L (Fig. 2) resulting in lower concentrations of mutagens available to interact with cytosolic DNA.[43] With respect to the mutagenicity of *N*-acyloxy-*N*-alkoxybenzamides, there is clearly an optimum log*P* value in the range of log*P*s covered by mutagens **12a–e**.

Several treatments are possible to generate QSARs catering for drugs covering a wide range of log*P*. To establish a QSAR that encompasses the activities of increasingly hydrophobic mutagens **12a–e**, we chose Kubinyi's bilinear model.[52,56–58] In Eqn 4, β is a non-linear term calculated by an iterative procedure. In cases where log*P* is sufficiently small, βP becomes negligible and therefore the $\log(\beta P + 1)$ term decreases to zero, converting the model to the linear form (Eqn 3). We determined that a $\log P_0$ of 6.4 is the optimum log*P* for activity and, by Kubinya's method, can be derived from log*P* and $\log(\beta P + 1)$ coefficients, *a* and *b*, from the regression analysis using Eqn 5.[52,56–58] Experimental and predicted LogTA100 from the bilinear model in Eqn 4 are given in Table 1 and are in good agreement when compared with the result from the linear model in Eqn 3. It will be reported in the section on 'Naphthalene as an intercalator' that a naphthalene

Table 1. LogP_{GC}, pK_a, experimental and calculated LogTA100 for **12a–e** and **13b**.

Compound	R, R′	Log*P*	pK_a	LogTA100				
				Exp.	Calc.[A]	Diff.[B]	Calc.[C]	Diff.[B]
12a	Hexyl, pentyl	5.18	4.86	3.42	3.37	−0.05	3.23	−0.19
12b	Heptyl, hexyl	6.02	4.78	3.25	3.59	0.34	3.38	0.13
12c	Octyl, heptyl	6.85	4.78	3.02	3.82	0.80	3.36	0.34
12d	Nonyl, octyl	7.69	4.78	2.95	4.05	1.10	3.12	0.17
12e	Decyl, nonyl	8.52	4.79	2.88	4.29	1.41	2.79	−0.09
13b	Octyl, heptyl	7.85	4.78	3.00	4.10	1.10	3.06	0.06

[A]Calculated according to linear Eqn 3.
[B]Calculated LogTA100 − experimental LogTA100.
[C]Calculated according to bilinear Eqn 4.

substituent increases binding to DNA through intercalation. As illustrated in Fig. 3, the activity of **13a** (closed diamond), given here for comparison,[40] is significantly higher than predicted, whereas that of the lipophilic **13b** is strongly suppressed (Fig. 3, open diamond). However, the activity of **13b** is well reproduced by Eqn 4, indicating that the activity enhancement due to the naphthamide structure is largely negated owing to lipid entrapment. K_L in Fig. 2 is dominant and limiting in this case.

$$\begin{aligned}\text{LogTA100} &= 0.243\,(\pm 0.02)\text{Log}P \\ &- 0.667\,(\pm 0.12)\text{Log}(\beta P + 1) \\ &+ 0.106\,(\pm 0.08)\text{p}K_a \\ &+ 0.088\,(\pm 0.03)E_s^1 \\ &+ 0.092\,(\pm 0.04)E_s^2 \\ &+ 0.022\,(\pm 0.05)E_s^3 + 1.466\,(\pm 0.41)\end{aligned} \quad (4)$$

$\text{Log}\beta = -6.639$, $n = 55$, $r^2 = 0.75$, adj. $r^2 = 0.71$, $s = 0.18$, $F = 19.7$; LOOCV $Q^2 = 0.60$.

$$\log_{10}P_O = \log_{10}[a/\beta(b-a)] \quad \text{(only for } b > a\text{)} \quad (5)$$

Steric effects on activity

Distal steric effects in triarylated mutagens bearing *tert*-butyl groups[59]

Steric effects would be expected to impact on activity levels in several ways; they could influence the capacity of NAAs to bind in the hydrophobic grooves of DNA (reducing K_M) or, in the bound state, they could inhibit reaction with nucleotides (reducing k_M). Previous investigations found that mono *tert*-butylated mutagens (**9**, X = Bu^t, **10**, Y = Bu^t, **11**, Z = Bu^t) were well predicted by an earlier QSAR.[59] Activity of the di-*tert*-butylated diaryl mutagen **14** (Chart 4) was also well predicted by the linear and bilinear QSARs in Eqns 3, 4 (Fig. 3, Table 2). For a series of di-*tert*-butylated triaryl mutagens **15a–c** and **16a** (Chart 4), we encountered significantly diminished activity with the linear QSAR in Eqn 3 (Fig. 3, filled circles, Table 2) and although dose responses were evident, with LogTA100 > 2, only **15c** can be regarded as mutagenic. No dose response could be obtained with tri-*tert*-butylated substrates **15d** and **16b**, which must be regarded as non-mutagenic towards TA100. We originally ascribed this reduced activity to the dimensions of these triarylated

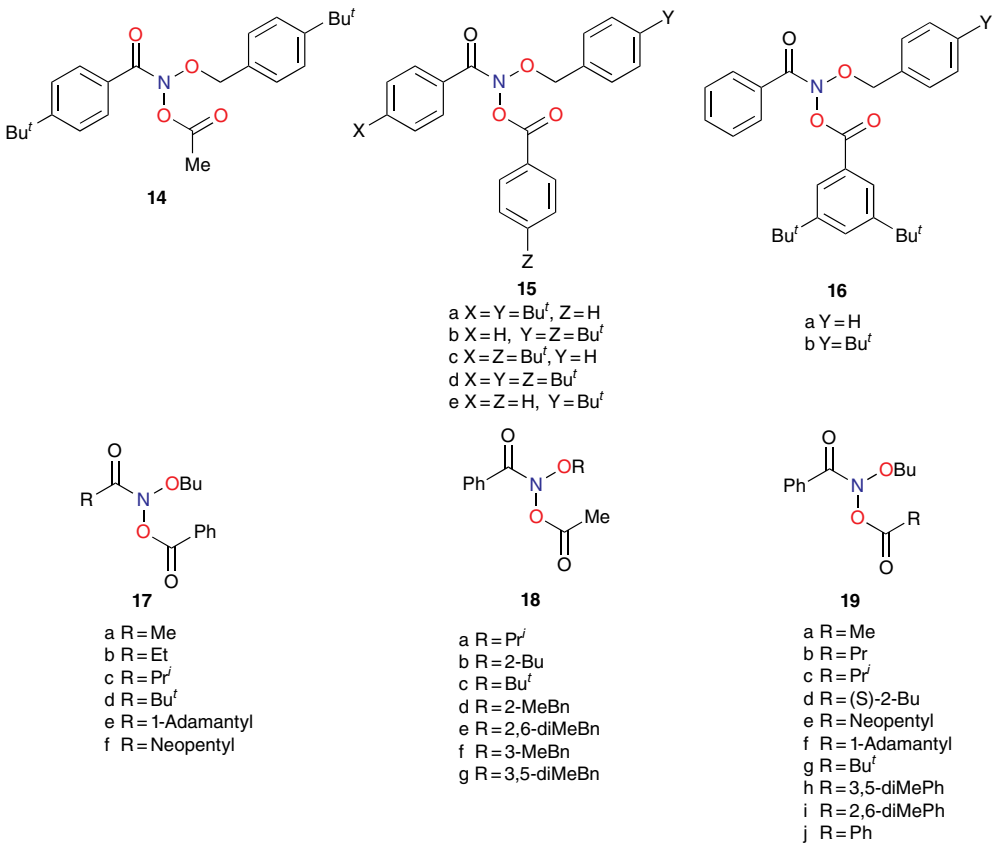

Chart 4. NAAs with varying spatial requirements on the acyl, alkoxyl and acyloxyl side-chains.

systems, which from X-ray and computed structures are from end to end between 14 and 17 Å, at least of the order of the width of the major groove of DNA (12 Å).[8,59] However, these substrates have log*P* values of 8.24, larger than the logP_0 for NAAs (logP_0 = 6.4). The bilinear QSAR in Eqn 4 corrects predicted values in relation to their high hydrophobicity and it is found that **15c** is well predicted (Table 2); the deviation from expected activity from Eqn 3 is entirely due to the increase in hydrophobicity in this case. On the other hand, activities of mutagens **15a–b** and **16a** still deviate strongly from predicted values after taking their increased hydrophobicity into account, which reinforces the groove exclusion argument for these substrates. As a *tert*-butylbenzyloxy group is common to all triarylated mutagens with greatly reduced activity, it would appear to be a limiting feature, whereas *tert*-butyl groups on the benzoyloxyl group may be less critical. From models, it is also possible that the transition state complex for S_N2 reaction at G-N7 can only be achieved with one *para tert*-butyl group.[8] Fig. 4*a* depicts the AM1-optimised transition state for the reaction of model *N*-formyloxy-*N*-methoxyformamide with G-N7. Modelling this into the major groove of a segment of DNA with **15e** (Fig. 4*b*) indicates severe restrictions for *tert*-butyl groups on the benzoyloxy and benzamide rings, which would need to make adverse contact with the wall of the major groove.

Proximal steric effects on the amide side chain[59]

Branching adjacent to the amide carbonyl in NAAs has a profound effect on the mutagenic response. Whereas acetamide **17a** is well predicted, propanamide **17b**, 2-methylpropanamide **17c**, 1-adamantanecarboxamide **17e** and neohexamide **17f** gave weak responses deviating significantly from the predicted activities from the linear QSAR in Eqn 3. Deviations from predicted values increased through the series CH_3 < Et < Pr^i < Bu^t. The *tert*-butyl side chain in **17d** resulted in no response at all. With adamantyl and neopentyl side chains (**17e** and **17f**), experimental activities deviated strongly from predicted activities (Fig. 5, filled diamonds; Table 3). The results are broadly in line with the rates of

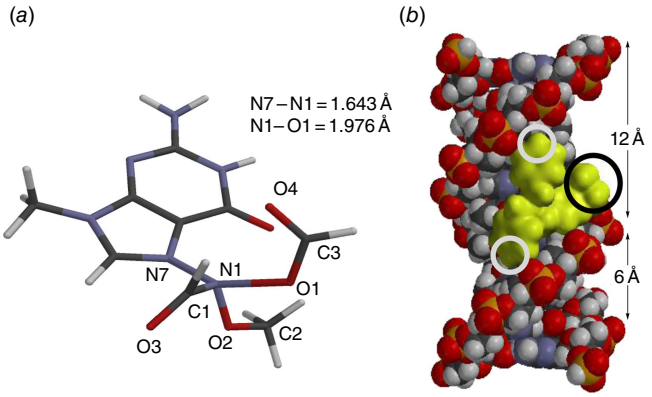

Fig. 4. (*a*) AM1 optimised transition state for reaction of *N*-formyloxy-*N*-methoxyformamide with G-N7; (*b*) Depicted in yellow is the conformation of **15e** in the major groove of DNA constrained to the transition state in (*a*) with side chains minimised by molecular mechanics (from Ref. [8]); black circle, *tert*-butyl group; white circles, *para* positions on the benzoyloxyl and benzamide side chains.

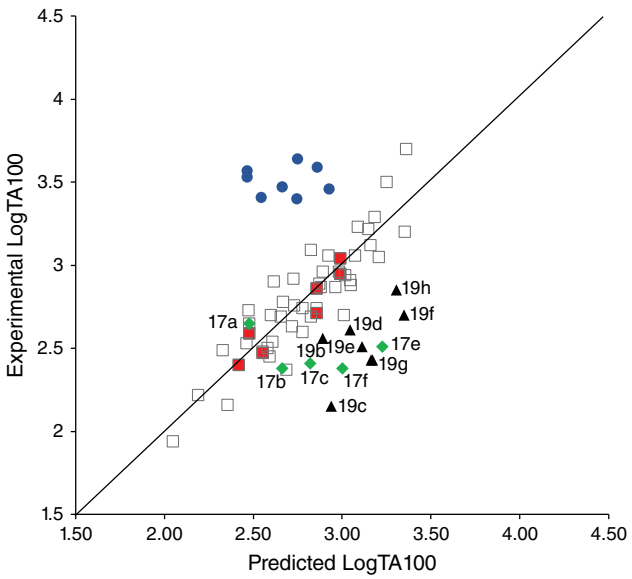

Fig. 5. Predicted vs experimental mutagenicities as LogTA100 for training set (open squares), **17a–e** (filled diamonds), **18a–g** (filled squares), **19a–i** (filled triangles) and **13a/20** (filled circles) in S. typhimurium TA100 using the linear QSAR in Eqn 3.

Table 2. LogP_{GC}, experimental and calculated LogTA100 for di-*tert*-butylated mutagens **14**, **15a–c** and **16a**.

Compound	Log*P*	LogTA100				
		Exp.	Calc.[A]	Diff.[B]	Calc.[C]	Diff.[B]
14	6.31	2.89	2.87	−0.02	2.9	0.01
15a	8.24	1.64	3.31	1.67	2.34	0.70
15b	8.24	1.86	3.41	1.55	2.54	0.68
15c	8.24	2.61	3.46	0.85	2.55	0.06
16a	8.24	2.07	4.13	2.06	2.86	0.79

[A]Calculated according to linear Eqn 3.
[B]Predicted LogTA100 − experimental LogTA100.
[C]Calculated according to bilinear Eqn 4.

Table 3. Rate constants for bimolecular reaction with *N*-methylaniline, logP_{GC}, pK_a, experimental and predicted LogTA100 for **17**, **18** and **19** using linear QSAR in Eqn 3.

Compound (R)	10^4 k^{303A}	Log*P*	pK_a	LogTA100		
				Exp.	Calc.[B]	Diff.[C]
17a Me	97.2	2.44	4.20	2.65	2.48	−0.17
17b Et	8.1	3.1	4.20	2.38	2.66	0.28
17c Pr^i	–	3.66	4.20	2.41	2.82	0.41
17d Bu^t	–		4.20	n.d.r.[D]	–	–
17e Ad	–	5.12	4.20	2.51	3.23	0.72
17f Neo	2.2	4.31	4.20	2.38	3.0	0.62
18a Pr^i	52	1.86	4.76	2.40	2.42	0.02
18b 2-Bu	38	2.07	4.76	2.59	2.48	−0.11
18c Bu^t	–	2.34	4.76	2.47	2.55	0.08
18d 2-MeBn	78	3.42	4.76	2.71	2.85	0.14
18e 2,6-diMeBn	26	3.91	4.76	3.04	2.99	−0.05
18f 3-MeBn	97	3.42	4.76	2.86	2.85	−0.01
18g 3,5-diMeBn	102	3.91	4.76	2.95	2.99	0.04
19a Me	414	2.44	4.76	2.50	2.58	0.08
19b Pr	122	3.51	4.82	2.56	2.89	0.33
19c Pr^i	91	3.66	4.85	2.15	2.94	0.79
19d (*S*)-2-Bu	97	4.08	4.80	2.61	3.05	0.44
19e Neopentyl	78	4.31	4.80	2.51	3.11	0.60
19f 1-Adamantyl	61	5.12	4.86	2.70	3.35	0.65
19g Bu^t	34	4.37	5.03	2.43	3.17	0.74
19h 3,5-diMePh	nd[E]	5.31	3.56	2.85	3.30	0.45
19i 2,6-diMePh	nd[E]	5.30	4.34	2.43	3.16	0.73
19j Ph	1844	4.34	4.20	2.7	3.01	0.31

[A]Rate constants for S_N2 reaction with *N*-methylaniline in [D_4]methanol.
[B]Calculated according to Eqn 3.
[C]Predicted LogTA100 − experimental LogTA100.
[D]No dose response.
[E]Not determined

S_N2 reactivity with *N*-methylaniline at 303 K in [D_4]methanol where amides with branched amide side chains in **17c**, **17d** and **17e** were unreactive (Table 3). Branching α to the carbonyl is also known to impede S_N2 displacement of chlorine in α′-haloketones.[60] Mutagenicity, which must involve reaction of DNA at G-N7, was observed, albeit weak in all but the 2,2-dimethylpropanamide substrate (**17d**). We have attributed this difference to a greater ease of S_N2 reaction in the hydrophobic groove of DNA; in solution, S_N2 transition states for reaction with amines are strongly charge-separated, resulting in large negative entropies of activation due to solvent reorganisation.[8,16–18] However, in the hydrophobic grooves of DNA, a similar transition state would not be adversely affected by negative entropy of activation, making S_N2 reactivity in the grooves of DNA easier than in solution. It is clear that in this series, mutagenic activity is limited by k_M in Fig. 2

Proximal steric effects on the alkoxyl side chain[61]

Branching adjacent to the alkoxyl oxygen and the presence of bulky benzyloxy groups in series **18** has almost no effect on mutagenic activity and the activity of all mutagens was well predicted by the linear QSAR in Eqn 3 (Fig. 5 – filled squares, Table 3). Their activities are controlled by their log*P* and pK_a values, which impact on K_M and k_M in Fig. 2. These are all small molecules, so groove binding would not be expected to be limiting and bulkiness at the alkoxyl group does not appear to impede S_N2 reactivity at G-N7. The rates

of S_N2 reactions with *N*-methylaniline in [D4]methanol have also been measured for this series and rate constants at 303 K are somewhat smaller than their straight-chain *n*-butoxy analogue **19a** (Table 3).[16] **18c**, with a *tert*-butoxy group, was unreactive but the steric interference is not as severe as is found with branching on the amide side chain, which we attribute to greater flexibility on the alkoxyl side chain. Clearly though, a reduction in the ease of S_N2 reactivity with branching does not manifest itself in the mutagenic response. Once again, the factors controlling reactivity in the hydrophobic grooves of DNA appear to be somewhat different from those governing S_N2 reactions with amines in solution.

Steric effects on the acyloxyl side chain[61]

A series of mutagens bearing bulky substituents adjacent to the acyloxyl carbonyl in **19** demonstrated a systematic suppression of the mutagenic activity relative to the predicted activities from Eqn 3 (Fig. 5, filled triangles; Table 3). All have small log*P* values and ought not to be subject to lipid entrapment or restricted access to the major groove. Although for a range of such compounds rates of reactivity with *N*-methylaniline correlated negatively with pK_a (Eqn 1),[16] mutagenic activities were suppressed by an average of 0.59 LogTA100. While mutagen **19a** with an acetoxyl leaving group (in training set) and to a degree **19b** with a butanoyloxyl group are predicted well, the effect of branching on LogTA100 as in **19c–g** is significant, with the interference of isopropyl (**19c**) and *tert*-butyl groups (**19g**) being the greatest. This reflects steric hindrance to reaction with DNA, possibly through inability to achieve a conformation suitable for reaction at G-N7 (lowering k_M in Fig. 2). It is possible that, unlike groups on the alkoxyl side chain, the acyloxyl group must make unavoidable contact with the wall of the major groove. A comparison of data for the benzoyloxy substrate **19j** with the dimethylated analogues reinforces this. Although **19j** was slightly overpredicted, the 2,6-dimethylphenyl side chain in **19i** strongly inhibits activity (Table 3). The effect is reduced when the methyl groups are on the 3- and 5-positions in **19h**. Clearly, in **19i** the twisting that would be required to minimise steric interference with the carbonyl must have an influence (Fig. 6).

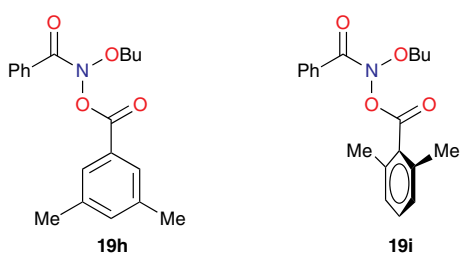

Fig. 6. Conformations in *N*-butoxy-*N*-(3,5-dimethylbenzoyloxy)- and *N*-butoxy-*N*-(2,6-dimethylbenzoyloxy)benzamides **19h** and **19i**.

Intercalation of fused polycyclic aromatics

Naphthalene as an intercalator

N-Acetoxy-*N*-butoxy-2-naphthamide mutagen **13a** was part of an earlier study in which we demonstrated an increased degree of DNA damage relative to other NAAs with similar log*P*.[38] Furthermore, **13a** exhibited mutagenic activity nearly an order of magnitude higher than predicted by the QSAR in Eqn 3 (Fig. 3, solid diamond).[40] This, together with a series of naphthalene-containing NAAs **20a–g** (Chart 5), all showed a remarkably consistent increased activity relative to predicted LogTA100 levels based on the QSAR in Eqn 3, with most differences between experimental and predicted activities close to 1 LogTA100 (Fig. 5, filled circles; Table 4).[42] Futhermore, the enhanced activity was evident irrespective of the regiochemistry, the locus of substitution on the naphthalene nucleus, or the length of aliphatic tethers where present. We attributed this enhancement to an increase in residence time on DNA through the capacity of the planar naphthalene to intercalate with the DNA bases.

Naphthalene has not generally been regarded as an intercalator, a property reserved for larger, fused polyaromatic systems with greater surface areas.[62–64] The ring system should possess a minimum of three rings to give an optimum surface area of more than 28 Å.[65] Various theories have been proffered regarding the capacity of planar aromatic systems to intercalate and the presence of positively charged side chains or acyl substitution was deemed important for naphthalene intercalation.[66,67] The intercalation of naphthalene mono- and di-imides, established threading intercalators, is well known.[68–70] Although in only two of the set studied, **13a** and **20a**, was naphthalene acyl-substituted, the remainder being bonded to methylene, it is hard to ascribe this increased activity to any process other than intercalation. These molecules have very modest computed log*P*s and no special features above those of similarly constituted benzamide systems in the training set. However, a modest, reversible ability to intercalate into DNA would increase residence time in the grooves of DNA, thereby increasing K_M in Fig. 2.

TA98 is a frameshift strain derived from *Salmonella typhimurium* that is used to detect intercalation. In effect a base deletion results in a reading error and a failure to proliferate in the plate media used in Ames assays. The space requirement for an intercalated polycyclic aromatic hydrocarbon (PAH) (3.4 Å) is similar to that required by a single base pair,[63,71–76] and intercalation of a PAH between the bases of DNA reinstates the wild-type reading frame in *S. typhimurium* through an $a + 1$ frameshift.[41,76,77] Furthermore, such restoration is particularly effective (10–100-fold increase) when the intercalative group is associated with an electrophilic centre, reaction through which can localise the intercalating group.[76–79] Importantly, where the

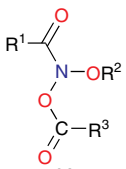

20

a R^1 = Me, R^2 = Bu, R^3 = 2-Np
b R^1 = Me, R^2 = Bu, R^3 = CH_2-2-Np
c R^1 = Me, R^2 = Bu, R^3 = $(CH_2)_2$-2-Np
d R^1 = Me, R^2 = CH_2-2-Np, R^3 = Me
e R^1 = Me, R^2 = $(CH_2)_2$-2-Np, R^3 = Me
f R^1 = Me, R^2 = $(CH_2)_3$-2-Np, R^3 = Me
g R^1 = Me, R^2 = CH_2-1-Np, R^3 = Me

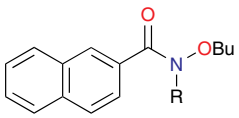

21

a R = OEt
b R = Me

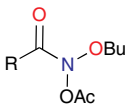

22

a R = 1-Fluorenyl
b R = 4-Fluorenyl
c R = 1-Fluorenonyl
d R = 2-Fluorenonyl
e R = 4-Fluorenonyl

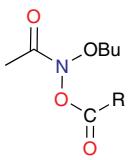

23

a R = 1-Fluorenyl
b R = 4-Fluorenyl
c R = 1-Fluorenonyl
d R = 2-Fluorenonyl
e R = 4-Fluorenonyl

Chart 5. NAAs with side chains bearing naphthalene **20**, fluorene and fluorenone (**22**/**23**) and related naphthamides (**21**).

Table 4. Experimental and predicted LogTA100 for **13a** and **20a–g** in *S. typhimurium* TA100 when calculated using linear QSARs in Eqns 3, 6, and bilinear QSAR in Eqn 7.

Mutagen	Exp.[A]	Linear QSAR Eqn 3		Linear QSAR Eqn 6 (I = 1)		Bilinear QSAR Eqn 7 (I = 1)	
		Pred.[B]	Diff.[C]	Pred.[B]	Diff.[C]	Pred.[B]	Diff.[C]
13a	3.59[D]	2.86	−0.73	3.68	0.09	3.65	0.06
20a	3.64	2.75	−0.89	3.58	−0.06	3.59	−0.05
20b	3.4	2.75	−0.65	3.57	0.17	3.58	0.18
20c	3.46	2.93	−0.53	3.74	0.28	3.72	0.24
20d	3.53	2.47	−1.06	3.31	−0.22	3.33	−0.20
20e	3.57	2.47	−1.10	3.31	−0.26	3.33	−0.24
20f	3.41	2.54	−0.87	3.39	−0.02	3.39	−0.02
20g	3.48	2.66	−0.82	3.50	0.02	3.49	0.01

[A]Experimental LogTA100.
[B]Predicted LogTA100.
[C]Predicted LogTA100 − experimental LogTA100.
[D]An average of LogTA100 = 3.62 and 3.56 values for **2** was used in derivation of Eqns 6, 7.

intercalator is dissociated in the reaction with DNA, the duality requirement is lost, resulting in a weak TA98 response. With their electrophilic amide nitrogens, NAAs appeared to be ideal candidates to effect such frameshifts. We subjected naphthalene-bearing mutagens **13a**, **20a**, **20d** and **20g** to TA98 tests and found linear dose responses and significant LogTA98 at 1 μmol per plate for **13a** (490 revertants; average of six tests), **20d** (287 revertants) and **20g** (114 revertants), which was not evident in the control systems *N*-acetoxy-*N*-butoxybenzamide **19a** and *N*-benzoyloxy-*N*-butoxyacetamide **17a**, the phenyl analogues of **13a** and **20a** or naphthalene-bearing systems without electrophilic nitrogen such as **21a–b**, both of which produced no dose response.[42] **20a**, where the intercalator dissociates from the mutagen in reaction with DNA, resulted, predictably, in a weak response (15 revertants) in TA98.

We consider this clear evidence for intercalation of naphthalene moieties.

To account for this activity enhancement, we regenerated a linear (Eqn 6) and a corresponding bilinear (Eqn 7) QSAR to enable prediction of this intercalative ability by the introduction of an indicator variable, I, which is given the value 1 if a naphthalene is present, otherwise 0.

$$\begin{aligned}\text{LogTA100} = {} & 0.26\,(\pm 0.03)\log P + 0.17\,(\pm 0.08)\text{p}K_\text{a} \\ & + 0.12\,(\pm 0.03)E_\text{s}^1 + 0.14\,(\pm 0.04)E_\text{s}^2 \\ & + 0.08\,(\pm 0.05)E_\text{s}^3 + 0.83\,(\pm 0.06)I \\ & + 1.12\,(\pm 0.41) \qquad (6)\end{aligned}$$

$n = 58$, $R^2 = 0.85$, adj. $R^2 = 0.83$, $s = 0.16$, $F = 48.2$; LOOCV $Q^2 = 0.85$.

$$\begin{aligned}\text{LogTA100} = {} & 0.23\,(\pm 0.02)\log P \\ & - 0.65\,(\pm 0.12)\text{Log}(\beta P + 1) \\ & + 0.11\,(\pm 0.08)\text{p}K_\text{a} + 0.09\,(\pm 0.03)E_s^1 \\ & + 0.09\,(\pm 0.04)E_s^2 + 0.01\,(\pm 0.05)E_s^3 \\ & + 0.85\,(\pm 0.07)I + 1.48\,(\pm 0.40) \qquad (7)\end{aligned}$$

$\text{Log}\beta = -6.705$, $n = 63$, $R^2 = 0.81$, adj. $R^2 = 0.79$, $s = 0.18$, $F = 29.6$; LOOCV $Q^2 = 0.76$.

From Eqn 5 and the coefficients in Eqn 7, a revised LogP_0 value of 6.44 can be calculated, slightly higher than 6.37 calculated from Eqn 3.

A comparison of QSAR results for **13a**, **20a–g** from Eqn 3 with those from revised linear and bilinear QSARs in Eqns 6, 7 using $I = 1$ is presented in Table 4. The differences between experimental and predicted mutagenicities are significantly diminished when compared with predictions from the linear QSAR in Eqn 3. Correlations between the predicted and experimental LogTA100, based on the new QSAR in Eqn 6, are illustrated in Fig. 7 (training set, filled squares).

As the correlations with log$P$ and I in Eqn 6 are highly significant (P- values of 10^{-13} and 10^{-17} respectively), the respective coefficients of 0.26 and 0.83 indicate that the attachment of one naphthalene group increases activity equivalent to between 3 and 4 log$P$. Although the log$P$ of **13a** and **20a–g** (log$P$ 2.0–3.8) falls below the logP_0 for NAAs (6.44 from Eqn 7), they exhibit mutagenic activity that is equivalent to mutagens with an 'effective' log$P$ ranging between log$P$ = 5 and 7. This can be readily seen from a plot of linear (Eqn 8) and bilinear log$P$ dependence (Eqn 9) over the range log$P$ = 0–10 (Fig. 8), where the boxes reflect actual and effective log$P$ for this series of naphthalene-bearing NAAs.[42]

$$\text{LogTA100} = 0.189\,(\pm 0.02)\log P + 2.078\,(\pm 0.08) \quad (8)$$

$n = 55$, $R^2 = 0.677$, $s = 0.19$, $F = 98.5$.

$$\text{LogTA100} = 0.209\,(\pm 0.02)\log P - 0.472\,(\pm 0.10)\log(\beta P + 1) + 2.02\,(\pm 0.08) \quad (9)$$

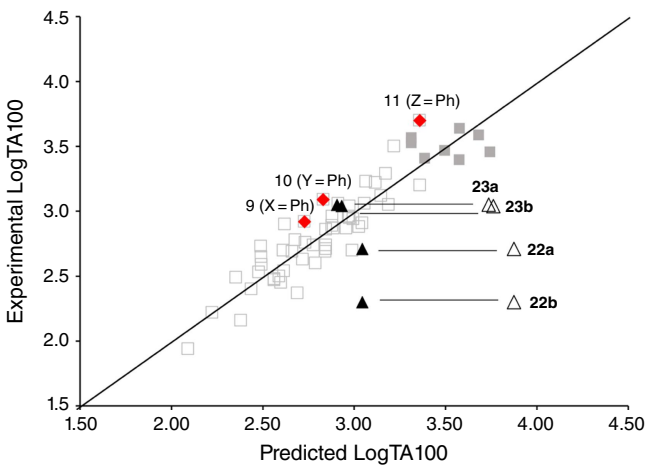

Fig. 7. Predicted vs experimental mutagenicities as LogTA100 for training set (filled and empty squares), biphenyl side chains (filled diamonds) and fluorene side chains **22a–b, 23a–b** (open triangles $I = 1$ and filled triangles $I = 0$) in S. typhimurium TA100 using the linear QSAR in Eqn 6.

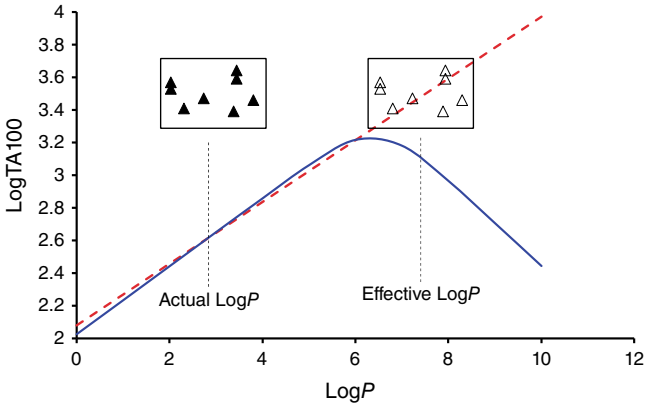

Fig. 8. Linear (Eqn 8) and bilinear (Eqn 9) dependence on logP and the experimental activities of naphthalene-bearing compounds **13a, 20a–g** at calculated (closed triangles) and effective logP range (open triangles).[42]

Log$\beta = -6.466$, $n = 55$, $R^2 = 0.677$, $s = 0.19$, $F = 35.55954$, log$P_0 = 6.37$.

This finding that a naphthalene enhances the activity of NAAs to the tune of between 3 and 4 log$P$ units by its hitherto unknown intercalative ability is an important new discovery. Presumably, the DNA targeting function of naphthalene is not unique to NAAs. The Lipinski Limit is a hydrophobicity above which lipid entrapment diminishes the activity of a drug.[55] A drug with log$P$ close to the Lipinski Limit for that type of drug, but bearing a simple naphthalene substituent, can pass through the lipid membrane, yet exhibit binding to DNA equivalent to a molecule with a substantially higher hydrophobicity.

Fluorene and fluorenone as intercalators[80,81]

The role of naphthalene appears not to be unique. We have recently found that Eqn 6 (log$P$ < 6.4) or Eqn 7 (log$P$ > 6.4) can be used to differentiate between molecular substructure capable of intercalation into DNA and substructure that does not intercalate, based on the fit of measured LogTA100 with $I = 1$ or 0. If the fit to the QSAR is best with $I = 0$, the structure is a groove binder with mode of action similar to most of the mutagens we have studied. If the fit is best with $I = 1$, such molecules target DNA through a degree of intercalation akin to that of naphthalene-bearing mutagens.

Three substructures demonstrate this principle: NAAs bearing the biphenyl moiety, the fluorene ring system and the fluorenone group, which are related. In fluorenes, the biphenyl rings are bridged by a methylene, making fluorene groups largely planar but not cross-conjugated as is the case of fluorenones, where the rings are bridged by a carbonyl (Chart 6).

Measurement of TA100 activity for NAAs with potential intercalators incorporated into side chains was instructive. Firstly, biphenyl systems on all three side chains (Fig. 7, filled diamonds) have previously been shown to conform to

linear QSARs and are part of the training set, which now incorporates eight naphthalene-bearing NAAs (Fig. 7, filled squares). The biphenyl group does not target DNA beyond its hydrophobic influence.

The activity of the four fluorene-bearing mutagens (Chart 7) is greatly over-predicted with $I = 1$ (Fig. 7, open triangles, Table 5).[80] Activities of **23a**, **23b** are well predicted and **22a** is adequately predicted with $I = 0$. Activity of **22b** would appear to be even lower than predicted with $I = 0$ (Fig. 7, filled triangles; Table 5). It would appear that all four NAAs bearing fluorene are not targeted to DNA through intercalation, as was the case with naphthalene. These structures possess an aliphatic bridge and no cross-conjugation, which may result in poor π–π stacking and a lack of polarisability. We ascribed the much diminished activity of **22b** to the fact that the pendant group is directed into the bay region of the fluorene, resulting in more difficult access to nucleophilic DNA components. The same is true for **23b** and both side chains would be twisted out of plane of the ring system. However, there is less flexibility in the pendant group in **22b**.

22b, **23a** and **23b** gave negative results in the TA98 screen. Surprisingly, **22a** gave a reasonably positive result (246 induced revertants at 1 μmol per plate) though it showed no enhancement in TA100 and in fact was underpredicted using the indicator variable $I = 0$. We have ascribed this to oxidation of the fluorene to the fluorenone **22c** in the plate incubation or, alternatively, selective metabolism to **22c** by bacterial *S. typhimurium* TA98.[80]

4-Aminobiphenyl and 2-aminofluorene are well known carcinogens where the metabolic route involves cytochrome P450 oxidation of the nitrogen, ultimately leading to electrophilic nitrenium ion formation, as illustrated in Scheme 2.[25–31] TA98 studies, and studies with other frameshift-sensitive strains, have implicated metabolites of these compounds as intercalators.[76,78] Our results point to the fact that such intercalation is a function of the binding of the derived metabolites, the aryl nitrenium ions. The biphenyl or fluorene aromatic ring systems do not appear to promote intercalation.

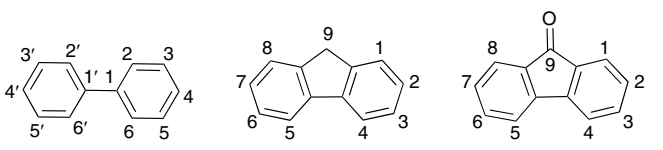

Chart 6. Relationship between biphenyl, fluorene and fluorenone structures.

Table 5. Experimental and predicted LogTA100 **22a–b**, **22d–e** and **23a–e** in *S. typhimurium* TA100 when calculated using linear QSAR in Eqn 6 with $I = 0$ and 1.

Mutagen[A]	LogTA100				
	Exp.	Pred. ($I = 0$)	Diff.[B]	Pred. ($I = 1$)	Diff.[B]
22a (1-Fl)	2.71	3.05	0.34	3.88	1.17
22b (4-Fl)	2.30	3.05	0.75	3.88	1.58
22d (2-Fn)	3.37	2.81	−0.56	3.65	0.28
22e (4-Fn)	2.62	2.81	0.19	3.65	1.03
23a (1-Fl)	3.04	2.93	−0.11	3.77	0.73
23b (4-Fl)	3.05	2.91	−0.14	3.74	0.69
23c (1-Fn)	3.57	2.59	−0.98	3.42	−0.15
23d (2-Fn)	2.64	2.65	0.01	3.49	0.85
23e (4-Fn)	2.57	2.58	0.01	3.42	0.85

[A]Fl, fluorene-bearing; Fn, fluorenone-bearing.
[B]Predicted LogTA100 − experimental LogTA100.

Fluorenone derivative **22c** could not be synthesised by existing protocols,[80,81] but the remaining fluorenone-bearing compounds (Chart 8) yielded a clearcut result. Activities of two of the fluorenone substrates, **22d** and **23c**, are clearly well predicted when $I = 1$ and those of the other three, **22e** and **23d–e**, are greatly overpredicted (Fig. 9, Table 5). However, activities of these three are very well predicted with $I = 0$.[80] Clearly, two of the NAAs bearing fluorenone, like naphthalene derivatives, benefit from intercalation, whereas the remainder do not.

Substitution at the 2- (in **22d**) and the 1-position (**23c**) appears to facilitate intercalation. In both these, the tricylic conjugated system can most probably penetrate adequately between base pairs. Of the three systems that did not report enhanced activity, **22e** and **23e** have the pendant active centre directed towards the distal ring in the bay region. In such systems, the intercalation would have to be *edge-on* rather than *end-on* and, presumably, would lead to a poor intra-base penetration and π–π stacking ability.

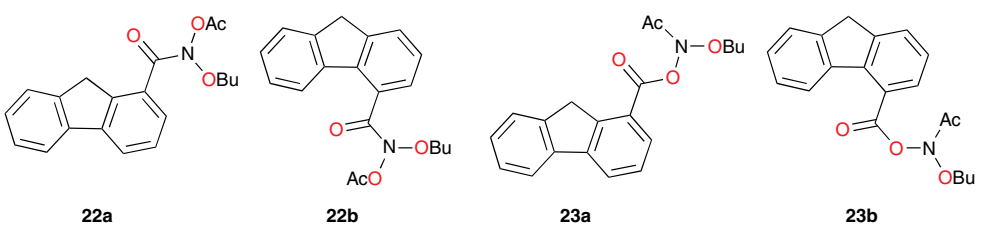

Chart 7. NAAs bearing fluorene on the acyl and acyloxyl side chains.

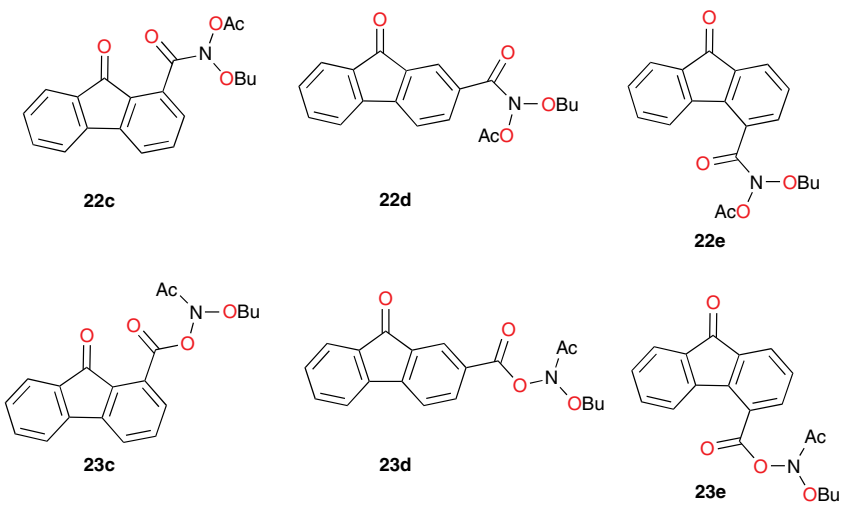

Chart 8. NAAs bearing fluorenone on the acyl and acyloxyl side chains.

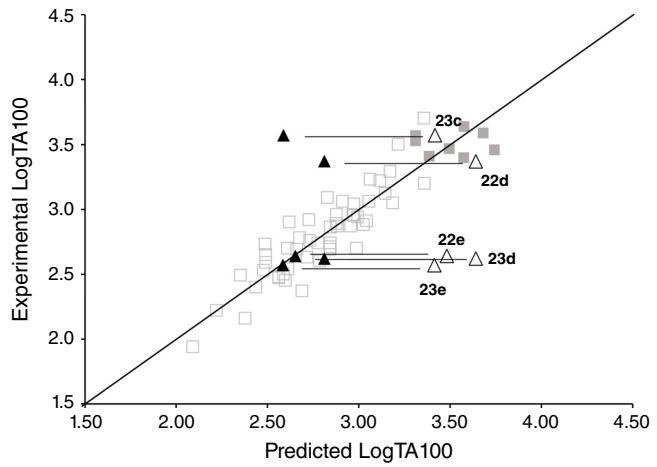

Fig. 9. Predicted vs experimental mutagenicities as LogTA100 for training set (filled and empty squares), fluorenone side chains **22d–e** and **23c–e** (open triangles $I = 1$, filled triangles $I = 0$) in *S. typhimurium* using the linear QSAR in Eqn 6.

23d appears *not* to intercalate even though it could do so in an end-on fashion. We have argued that the difference between **23d** and intercalating **22d** may lie in different electronic effects owing to the fact that in **23d**, the fluorenone is bonded through the 2-position to the ester carbonyl whereas in **22d**, it is bonded to the amide carbonyl although the argument is by no means a compelling one.[80]

Fig. 10 shows AM1-optimised ground state geometries for **22c–e** and **23c–e**. It is clear, when comparing **22d** with **22e**, and also **23c** with **23e** that the accessible surface area of the tricyclic systems in **22e** and **23e**, where the pendant group is in the bay region, would be smaller than in **22d** and **23c**, which can bind in an end-on fashion.

TA98 studies confirmed that in keeping with its TA100 result, **22d** is a strong intercalator (TA98 = 1458 revertants at 1 μmol per plate).[80] In accord with the dissociation arguments above, **23c** (a strong intercalator from TA100 studies) gave a weak response through disconnection on reaction, as did **22e** and **23d–e**, which were not predicted to intercalate by TA100. Though we were unable to synthesise **22c**, it is possible that it was generated from fluorene **22a** by oxidation during the TA98 procedure.

1-Substituted naphthalenes and intercalation

Application of our QSAR would appear to differentiate not only between substructure promoting intercalation or otherwise, but also between modes of intercalation. A study of the mutagenic activity of five other mutagens bearing a 1-naphthalene group (Chart 9) reinforced this concept. Although **24b** could not be synthesised owing to steric impact of the 2-methyl group, LogTA100 data for five naphthalene-bearing mutagens **24a**, **24c** and **25a–c** were acquired.[81]

The activities of **24a** and **25b** and **25c** were clearly overpredicted from Eqn 6 with $I = 1$ (Fig. 11, open triangles; Table 6), but were not in excess of the predicted value with $I = 0$ (Fig. 11, closed triangles; Table 6). Such naphthalenes would need to intercalate in an edge-on rather than an end-on orientation as the pendant groups would be twisted out of the plane of the ring system, thereby blocking penetration of the naphthalene ring in a substantive fashion.[81]

25a gave a reproducible ambivalent result while **24c** surprisingly and reproducibly correlated with $I = 1$. Of the five mutagens bearing 1-substituted naphthalenes, only **24c** was active in TA98 (3803 revertants at 1 μmol per plate), confirming the TA100 study.[81] Although this was a seemingly incongruous result, there is some evidence from PAH intercalation that a methyl substituent can enhance intercalation, possibly by increasing polarisability of the ring system and enhancing electrostatic interactions and π–π stacking capability.[82] It is deemed that the electronic influence of aliphatic substituents that enhance intercalation are more important than the steric effects that inhibit intercalation.

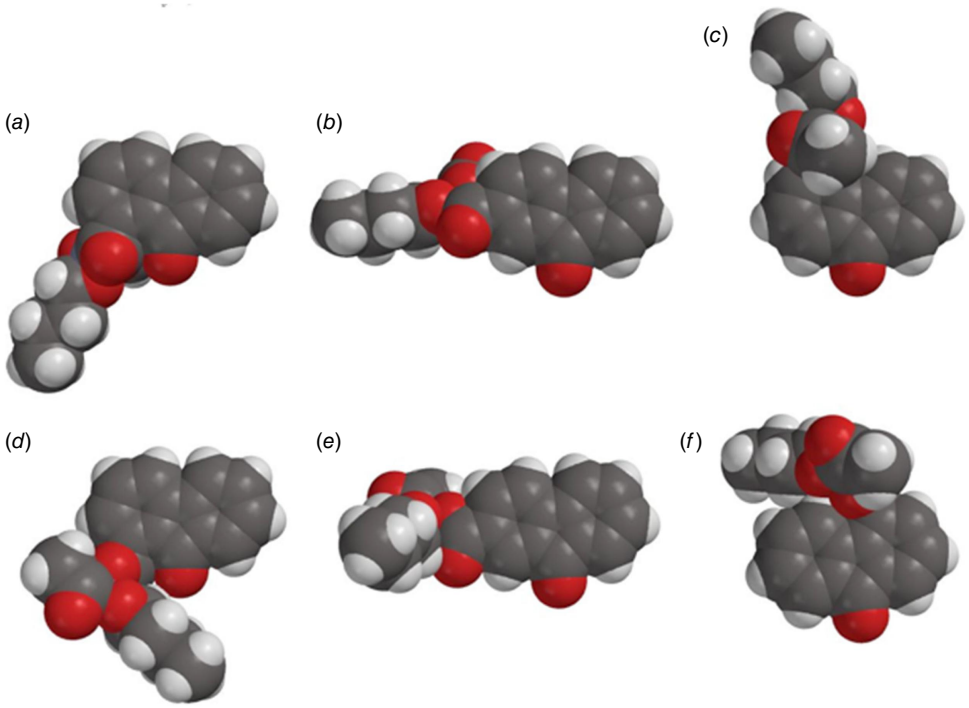

Fig. 10. AM1 minimum energy conformations of (*a*) **22c**, (*b*) **22d**, (*c*) **22e**, (*d*) **23c**, (*e*) **23d** and (*f*) **23e**.

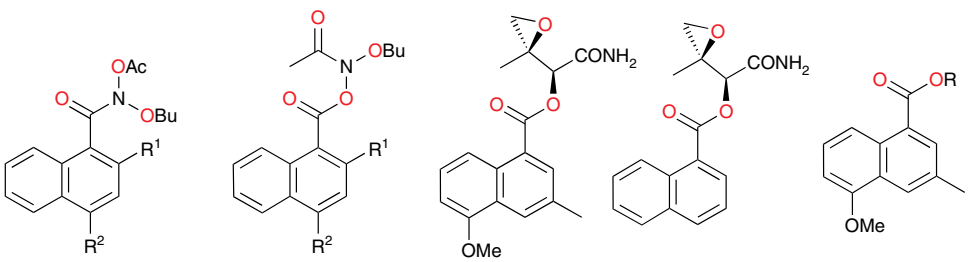

24

a $R^1=R^2=H$
b $R^1=Me$, $R^2=H$
c $R^1=H$, $R^2=Me$

25

a $R^1=R^2=H$
b $R^1=Me$, $R^2=H$
c $R^1=H$, $R^2=Me$

26 **27**

28

a R=H
b R=Me

Chart 9. NAAs bearing 1-naphthyl groups on the acyl and acyloxyl side chains and related Azinomycin B substructures.

There is fairly recent evidence that derivatives of the 'left half' of Azinomycin B modified to remove alkylating activity, **26**, and that have an acyl side chain naphthalene motif similar to that of **25** bind intercalatively to DNA.[83] However, the unsubstituted naphthalene system in the same structure **27** was shown to be ineffective in DNA binding.[83] The impacts of substituents on π-electron density distribution are likely to make a significant contribution to the intercalative potential of the naphthalene group. It is not a clearcut situation though; computational studies by Alcaro *et al.* have been unable to clearly define the role of the naphthalene moiety in Azinomycin,[84,85] and Coleman *et al.*[86,87] and Casely-Hayford[88] suggest that there is no intercalation of the naphthalene moiety in **26** or **28**. There is no doubt, though, that **24c** intercalates and so too does **20g** with a 1-naphthyl group on the alkoxyl side chain (Table 4).

Once again, the difference between end-on and edge-on intercalative ability can clearly be seen in a comparison between the AM1-optimised structures of **13a** and **20a**, both 2-naphthalene derivatives, and their 1-naphthalene analogues **24a** and **25a** (Fig. 12).

Pyrene as an intercalator

Pyrene and its derivatives have long been known to bind to double-stranded DNA by intercalation and the property has been studied in detail through spectroscopic studies or binding studies.[89–95] Recently, kinetic studies have shown that the binding of a pyrene unit to DNA involves a two-step

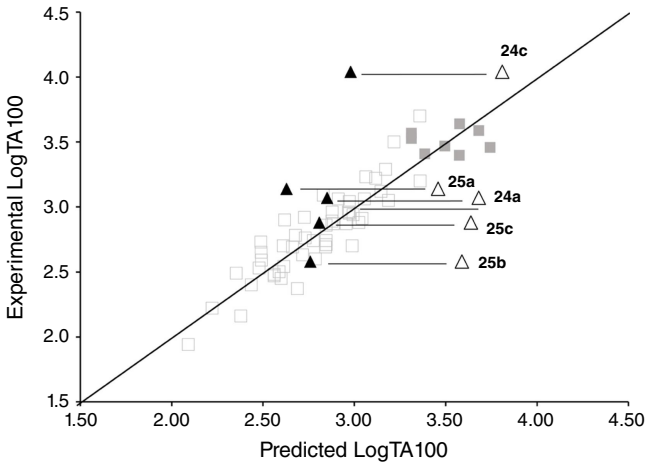

Fig. 11. Predicted vs experimental mutagenicities as LogTA100 for training set (filled and empty squares), 1-naphthalene side chains **24a**, **24c** and **25a–c** (open triangles $I = 1$, filled triangles $I = 0$) in *S. typhimurium* using the linear QSAR in Eqn 6.

Table 6. Experimental and predicted LogTA100 for **24a**, **24c** and **25a–c** in *S. typhimurium* TA100 when calculated using linear QSAR in Eqn 6 using $I = 1$ and 0.

Mutagen	LogTA100				
	Exp.	Pred. ($I = 0$)	Diff.[A]	Pred. ($I = 1$)	Diff.[A]
24a	3.07	2.85	−0.22	3.69	0.62
24c	4.04[B]	2.98	−1.06	3.81	−0.23
25a	3.09[C]	2.63	−0.46	3.46	0.37
25b	2.58	2.76	0.18	3.59	1.01
25c	2.88	2.81	−0.07	3.64	0.76

[A]Predicted LogTA100 − experimental LogTA100.
[B]Average data from two tests (LogTA100 = 4.06 and 4.01).
[C]Average data from two tests (LogTA100 = 3.04 and 3.14).

mechanism; the first step is the formation of a precursor complex, while the second step is the formation of the intercalated complex through penetration of the pyrene moiety between the base pairs of DNA.[90] Recently, the intercalation of a pyrene unit has been exploited as a photophysical probe,[93] in single-molecule atomic force microscopy (AFM) for double-stranded DNA mismatches,[96] and as a surface modification for the immobilisation of double-stranded DNA (ds-DNA) on a solid support.[91]

The capacity for pyrene to intercalate with ds-DNA with high binding constants spurred us to extend our QSAR work to NAAs bearing a pyrene substituent. On the premise that pyrene would localise the NAAs and the pendant electrophilic centre would need to access proximal guanines, 1-pyrene was attached directly and through a variable-length tether with a view to determining the impact of pyrene, or tethered pyrene, on mutagenic activity (Chart 10).

Table 7 gives experimental and predicted LogTA100 for pyrene-bearing mutagens, all of which have log*P* below 6, and the data are illustrated in Fig. 13. Four of the derivatives, **30a**, **31**, **32a** and **32b**, are better predicted with $I = 1$ (open triangles), although **30a**, bearing a pyrene tethered through one methylene group on the amide side chain, is still underpredicted with $I = 1$. This was the most mutagenic of all the NAAs we have tested. Surprisingly, LogTA100 for **30b** and **29** were better predicted with $I = 0$ although activities of both are somewhat overpredicted even with $I = 0$. **30a** and **30b** both bear the pyrene on the amide side chain but the propyl tether in **30b** appears to render activity typical of a groove binder rather than an intercalator. All three substrates with pyrene on the acyloxyl group (**31**, **32a** and **32b**) are predicted to benefit from intercalation. **30a** (9448 revertants at 1 μmol per plate), **31** (239 revertants at 1 μmol per plate) and **32a** (385 revertants at 1 μmol per plate) gave a positive result in TA98, confirming their intercalative ability whereas **30b** was negative in the TA98 test in accord with it reacting as a groove binder.

With pyrene-substituted mutagens, several scenarios are possible.

- The pyrene could intercalate strongly, in which case the tether must be of suitable length to enable reaction at an N7 of an adjacent or distal guanine. Should this occur, the mutagen would register as benefiting from enhanced activity in TA100 and as a frameshift mutagen in TA98 through localisation of the pyrene. It would appear that **30a**, **31** and **32a** fall into this category. Two of these (**30a** and **31**) bear a three-bond tether while **32a** has a four-bond tether.
- A mutagen could intercalate through pyrene but be unable to react at an adjacent or distal guanine. Intercalation is an equilibrium process, and such compounds could still damage DNA in a groove-bound situation and would register in TA100 with $I = 0$. However, they could also register as an intercalator in the TA98 test. **29** with a short, two-bond tether falls into this category. From Eqn 6, it correlates well with $I = 0$ but is moderately active in TA98 (281 revertants at 1 μmol per plate).
- A mutagen could intercalate and facilitate a reaction of the tethered nitrogen at a proximal or distal G-N7 but if the tether becomes disconnected in the process, which, as described earlier, is the case where the pyrene is on the acyloxyl side chain, the pyrene may not localise sufficiently without the tether, and register weakly in TA98. **32b** may fall into this category. The six-bond tether may inflict damage, probably at a distal G-N7, in the intercalated state and register as an intercalator in TA100 but disconnection through reaction at G-N7 results in poor pyrene retention; **32b** is negative in TA98 (26 revertants at 1 μmol per plate)
- A mutagen could register negatively for intercalation in both TA100 and TA98 if it reacts readily in the groove-bound state prior to intercalation but in the bonded state

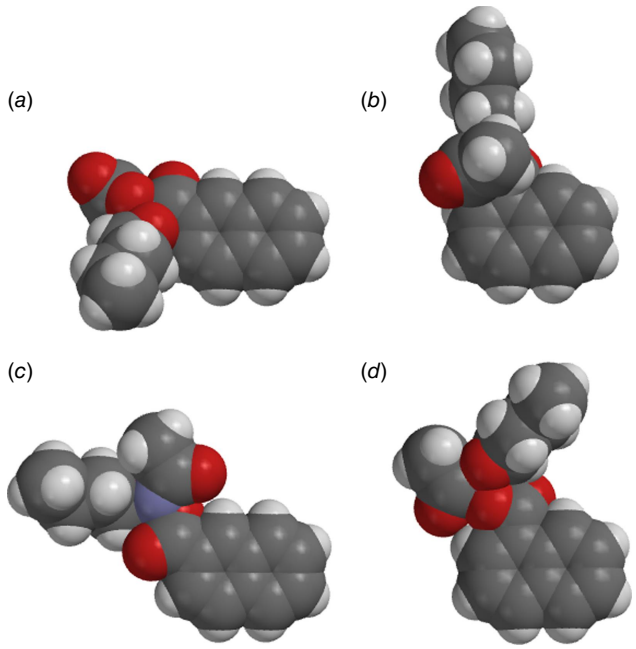

Fig. 12. AM1 optimised structures of 1- and 2-substituted naphthalene-bearing mutagens (*a*) **13a**, (*b*) **24a**, (*c*) **20a** and (*d*) **25a**.[81]

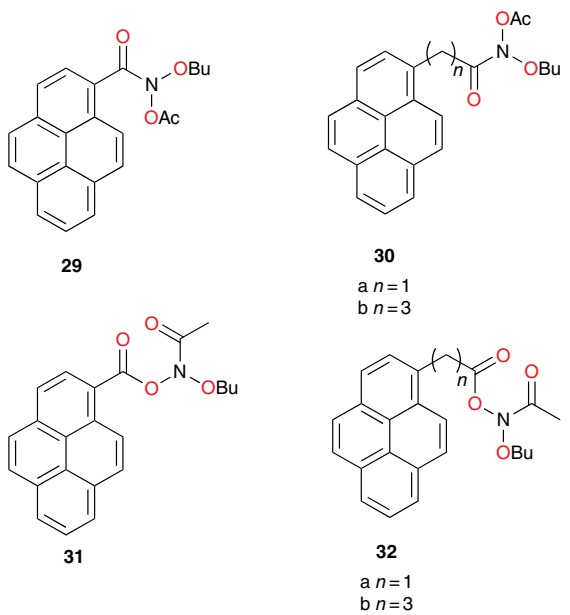

Chart 10. NAAs bearing pyrenyl groups on the acyl and acyloxyl side chains.

intercalation is difficult to achieve. **30b** could be categorised as such. Its activity in TA100 does not benefit from intercalative enhancement and it is a very poor intercalator from TA98 (88 revertants at 1 μmol per plate).

Molecular modelling suggests that with a three-bond tether, an intercalated pyrene would be able to react at an adjacent guanine without severe disruption to the helix. Hence, **30a** and **31** are of the most active forms.

Overall, though, throughout our investigations of intercalative ability, we have found that the result from the frameshift mutation strain TA98 was in agreement with the predictions from point mutation strain TA100 in 79% of the 24 compounds studied. In the majority of cases, those compounds showing enhanced TA100 mutagenicity were also mutagenic in TA98. In general, when $I = 0$, the mutagen was non-mutagenic in TA98, whereas with $I = 1$, the mutagen gave a positive result. Collectively, this adds credibility to the value of the indicator variable I being a reporter of intercalative ability of a PAH in the TA100 reverse mutation assay.[81]

Table 7. Experimental and predicted LogTA100 for **29**, **30a–b**, **31**, **32a–b** in *S. typhimurium* TA100 when calculated using the linear QSAR in Eqn 6 with $I = 0$ and 1.

Mutagen	LogTA100				
	Exp.	Pred. ($I = 0$)	Diff.[A]	Pred. ($I = 1$)	Diff.[A]
29	2.64	3.15	0.51	3.99	1.35
30a	4.49	3.14	−1.35	3.97	−0.52
30b	2.87	3.36	0.49	4.19	1.32
31	4.01	2.93	−1.08	3.76	−0.25
32a	3.88	3.06	−0.82	3.89	0.01
32b	4.10	3.36	−0.74	4.19	0.09

[A]Predicted LogTA100 − experimental LogTA100.

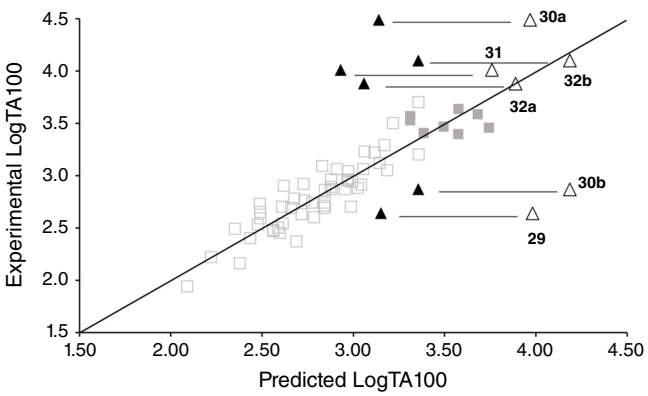

Fig. 13. Predicted vs experimental mutagenicities as LogTA100 for training set (filled and empty squares), pyrene-bearing *N*-acyloxy-*N*-alkoxyamides **29–32**; (open triangles $I = 1$, filled triangles $I = 0$) in *S. typhimurium* using the linear QSAR in Eqn 6.

Predictive power of QSAR

Activation by 4-nitrobenzyl substituents

Early studies of substituent electronic effects for a series of *N*-acyloxy-*N*-benzyloxybenzamides **10** produced a result

that at the time was little understood.[40] Activity for *N*-acetoxy-*N*-(4-nitrobenzyloxy)benzamide **33** in TA100 was substantially greater than expected but much lower in the presence of S9 liver homogenate, which is used to reproduce enzymic metabolic activation in the Ames test.[41] We subsequently investigated four other 4-nitrobenzyl-bearing NAAs, **34–37**, as well as the 2-nitro- and 3-nitro- analogues of **33**, **38** and **39** (Chart 11) (unpublished data, SA Glover, K Kavanagh, RR Schumacher).[81]

The results in Table 8 can be summarised as follows:

- Although the activity of **33** in the absence of S9 was extremely high, the activity in the presence of S9 appeared to be well predicted by Eqn 6.
- To varying degrees, the activities of all 4-nitrobenzyl-substituted NAAs **34–37** in the absence of metabolic activation are greater than predicted by Eqn 6, pointing to a general model for their mutagenicity.
- The activity of the 3-methylated derivative **37** is underpredicted by Eqn 6, but not to the same extent as **33.**
- The 2- and 3-nitro analogues **38** and **39** were suitably predicted by Eqn 6.

We contend that the heightened activity of the 4-nitrobenzyl substrates **33–37** is most likely due to reduction of the nitro group to the hydroxylamine by nitro reductase present in bacterial TA100 (Scheme 3). Acetylase or sulfotransferase would lead to the ester or sulfate ester derivatives, which could react with DNA or solvolyse to an electrophilic phenylnitrenium ion, though these ions are predicted to have very short lifetimes in aqueous media.[30–33] Debnath *et al.* invoked these pathways in correlating the activities of a wide range of nitro aromatics in TA100 without metabolic activation.[46,97] Clearly, log*P* can relate to binding to nitroreductase or sulfotransferase as well as to DNA. In the case of **33** in the presence of S9, the cytochrome P450 oxidative enzymes most likely preserve the integrity of the nitro group. Hence, the LogTA100 in the presence of S9 is almost identical to the predicted value (Table 8). We demonstrated early on that S9 plays no role in the activity of NAAs and, in general, dose–response plots were extended linearly where toxicity was demonstrated at higher doses without S9.[40]

The 2- and 3-nitrobenzyl configurations **38** and **39** are well behaved, with LogTA100 close to the predicted value based on Eqn 6. It is apparent that in these cases, nitro reductase would appear to be inactive, which may be due to poor host–guest interactions relative to *para*-substituted benzyl groups in **33–36**.

The 3-methyl-4-nitro analogue **37** appears not to be as mutagenic as **33** even though computations show that the nitro group in such configurations deviates minimally from planarity with the ring. This parallels the mutagenic activities of 4-nitrobiphenyl and its 3-methyl analogue, both of which require reduction and activation according to Scheme 3.[98] Boche showed that the reduced mutagenicity of the methylated derivative was more than likely due to interference with binding to nitroreductase in TA100 rather than disruption of coplanarity with the aromatic ring.[98,99]

Results for the naphthamide **36** indicate that, while the naphthyl group is present, it does not enhance activity through intercalation; LogTA100 is overpredicted with

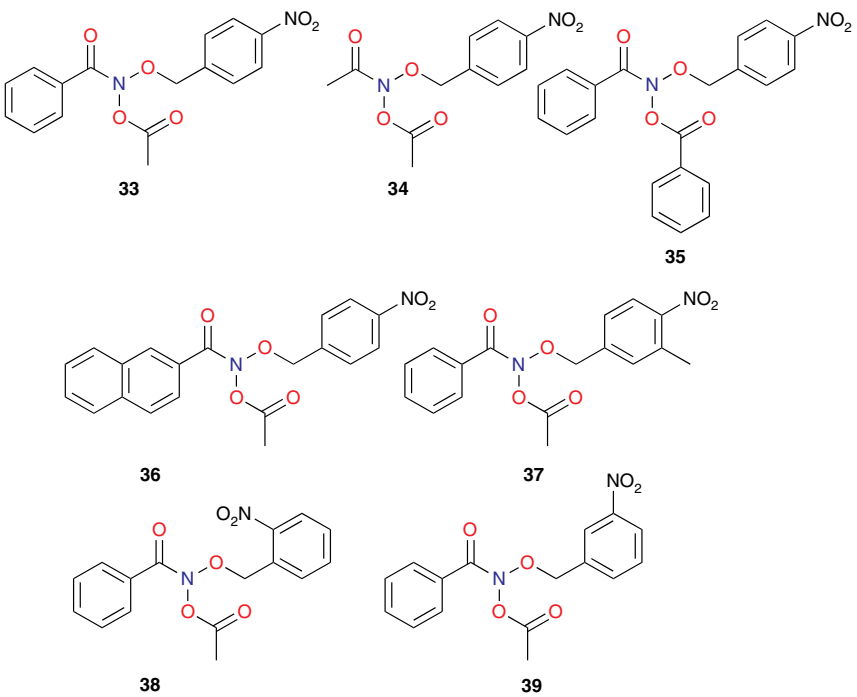

Chart 11. NAAs bearing nitrobenzyloxyl groups.

Table 8. Experimental and predicted LogTA100 for **33**–**39** in *S. typhimurium* TA100 when calculated using Eqn 6.

Compound	LogTA100		
	Exp.	Pred.	Diff.[A]
33 (−S9)	3.69	2.48	−1.21
33 (+S9)[B]	2.55	2.48	−0.07
34	3.26	1.98	−1.28
35	3.44	2.88	−0.56
36 ($I = 0$)	3.11	2.74	−0.37
36 ($I = 1$)	3.11	3.58	0.47
37	3.15	2.61	−0.54
38	3.01	2.73	−0.28
39	2.85	2.73	−0.12

[A]Predicted LogTA100 − experimental LogTA100.
[B]Previously obtained data presented for comparison.[40]

$I = 1$. With $I = 0$, the activity is significantly underpredicted as is the case for the other systems bearing a 4-nitrobenzyl group.

Activation of the 4-nitro substituent would appear not to be a uniform process across **33**–**37**, which among other things could reflect different binding capacities with reductive enzymes in TA100. However, the molecules have capacity to react through two modes, leading to moderately enhanced activities relative to predicted levels.

The role of bis-naphthalene substitution

Prior to development of functional QSARs governing the mutagenic activity of NAAs, Clay synthesised two NAAs bearing two naphthalene substituents, for which we obtained mutagenicity data (unpublished data, AM Bonin, SF Clay, SA Glover).[81] Although a single naphthalene has been shown to elevate activity through intercalation, the role of multiple naphthalene units in the same molecule was unknown. **40** and **41** (Chart 12) were synthesised with the expectation that the presence of two naphthalene units would further elevate activity relative to mutagens bearing one naphthalene. The log*P* values of **41** (log*P* 6.17) approached the logP_0 for NAAs (logP_0 6.4) and application of both the linear and bilinear QSARs was appropriate.

From Table 9, it is apparent that neither mutagen exhibited activity in keeping with intercalative enhancement; differences between predicted and experimental LogTA100 values were small when activities were computed with $I = 0$ by both Eqns 6, 7. Both **40** and **41** behave as if they are groove binders and the activity is largely governed by their hydrophobicity. Although these are fairly large molecules, normal reaction with G-N7 in the major groove of DNA would appear to operate. Intercalation of either naphthalene must be prohibited by these configurations; intercalation of one planar group must inhibit reaction with a neighbouring guanine, presumably for steric reasons. Hence, reaction must occur in a groove-bound complex without intercalation.

It should be mentioned that dual intercalation is prohibited by the neighbouring exclusion principle, which states that, at most, intercalators can only bind every second possible base pair site and binding of additional intercalators adjacent to the first is prohibited.[63,71] Owing to the changes in the DNA backbone conformation associated with the helix unwinding that is involved in the base pair separation essential for intercalation, there are significant limitations on the proximity of intercalation sites to one another. Bis-naphthyl NAAs have both intercalator units within relatively close proximity to one another; thus, even if one naphthalene unit were capable of intercalative binding, the other naphthalene would be prohibited by the interaction of the first.

Potential mutagenicity of a new *N*-acyloxy-*N*-alkoxyamide reagent for skeletal editing

A recent paper by Levin and coworkers in *Nature* described a method of editing nitrogen from secondary benzylic amines and related systems.[100] The method is widely applicable to editing nitrogen from secondary amines and suitably constituted primary amines.[101] The reaction employs a novel NAA, *N*-benzyloxy-*N*-pivaloyloxy-4-(trifluoromethyl)benzamide **42** (Scheme 4). Based on our precedent,[102–104] **42** reacts with suitable secondary amines, **43**, to produce an anomeric amide intermediate **44**, which undergoes HERON rearrangement to give benzyl 4-(trifluoromethyl)benzoate **45** and a 1,1-diazene or amino nitrene **46**. The reaction sequence was based on our discovery of both reactivity of NAAs with *N*-methylaniline,[8,16–19,50,59,105] and our discovery of the

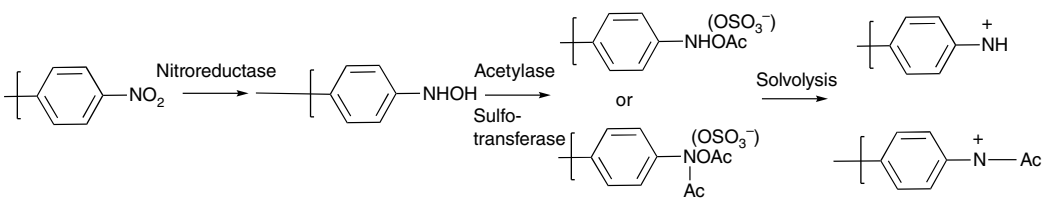

Scheme 3. Metabolic activation pathways of 4-nitrobenzyloxy systems in TA100.

HERON reaction.[13,102–105] The 1,1-diazene **46** extrudes nitrogen, producing two alkyl radicals, one of which is conjugated, and solvent cage recombination yields alkane **47**. Through this sequence, dibenzylamines generate bibenzyls in good yields, thereby editing nitrogen from the secondary amine.

The merit of Levin's reaction and the value of the reagent has been recognised by both Unsworth[106] and Bräse.[107] Importantly, however, Bräse cautioned that we had much earlier proved NAAs to be chemical mutagens, a fact seemingly overlooked by Levin and coworkers. The author apprised *Nature* of potential mutagenicity of **42** and a correction to the paper appeared addressing this fact and stating that **42** belongs to the class of NAAs 'some of which have been found to mutate genetic material'. However, the aforementioned sections indicate that almost all NAAs are classified as mutagenic; of the 100 variants we have made, only five structures were found not to be mutagenic in the Ames test.

Recently, we expanded our QSAR based on all published mutagens to date. Incorporation of three fluorene-bearing (**22a** and **23a–b)** and five fluorenone-bearing mutagens (**22d–e** and **23c–e)** yields Eqn 10:

$$\begin{aligned}\text{LogTA100} &= 0.24\,(\pm 0.03)\log P \\ &+ 0.09\,(\pm 0.06)\text{p}K_a + 0.10\,(\pm 0.03)E_s^1 \\ &+ 0.11\,(\pm 0.04)E_s^2 + 0.06\,(\pm 0.05)E_s^3 \\ &+ 0.83\,(\pm 0.06)I + 1.55 \end{aligned} \quad (10)$$

$n = 67$, $R^2 = 0.84$, adj. $R^2 = 0.82$ $s = 0.17$, $F = 50.7$; LOOCV $Q^2 = 0.83$.

The predictive power of this QSAR, which applies to NAAs with log$P < 6.4$,[52] is demonstrated by the small standard error, high F-value and the LOOCV Q^2 index of 0.83. Eqn 10 is similar to the preceding Eqn 6.[42,61]

Our QSAR allows us to predict mutagenic activity of congeners with some accuracy, and employing the QSAR in Eqn 10 indicates that **42** has a very high probability of being a direct-acting mutagen. Initial application of the QSAR to **42** predicts a very high level of mutagenic activity (LogTA100 = 3.14, Fig. 14). From our studies of steric effects on the acyloxyl side chain in substrates **19a–g**, we reported that branching at the α-position and other bulky groups reduces activity. Based on Eqn 10, the average suppression was 0.55 LogTA100 (Fig. 14, filled triangles).[61]

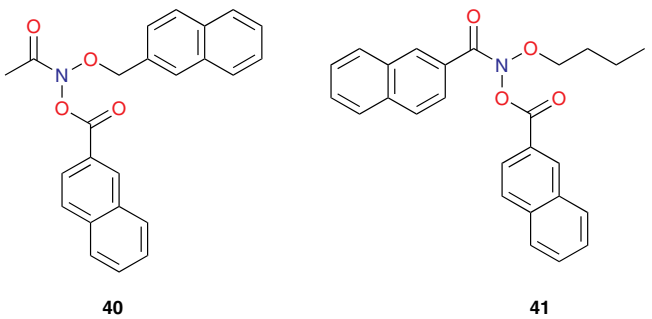

40 **41**

Chart 12. NAAs bearing two 2-naphthalene substituents.

Table 9. Experimental and predicted LogTA100 for **40** and **41** in *S. typhimurium* TA100 when calculated using the linear QSAR in Eqn 6 and bilinear QSAR in Eqn 7 with $I = 0$ and 1.

Mutagen	LogTA100				
	Exp.	Pred. ($I = 0$)[A]	Diff.[A,B]	Pred. ($I = 1$)[A]	Diff.[A,B]
40	3.29	3.14 (3.08)	−0.15 (−0.21)	3.97 (3.93)	0.68 (0.64)
41	3.18	3.46 (3.30)	0.28 (0.12)	4.30 (4.15)	1.12 (0.97)

[A]Data calculated using Eqn 6; bilinear data from Eqn 7 in parentheses.
[B]Predicted LogTA100 − experimental LogTA100.

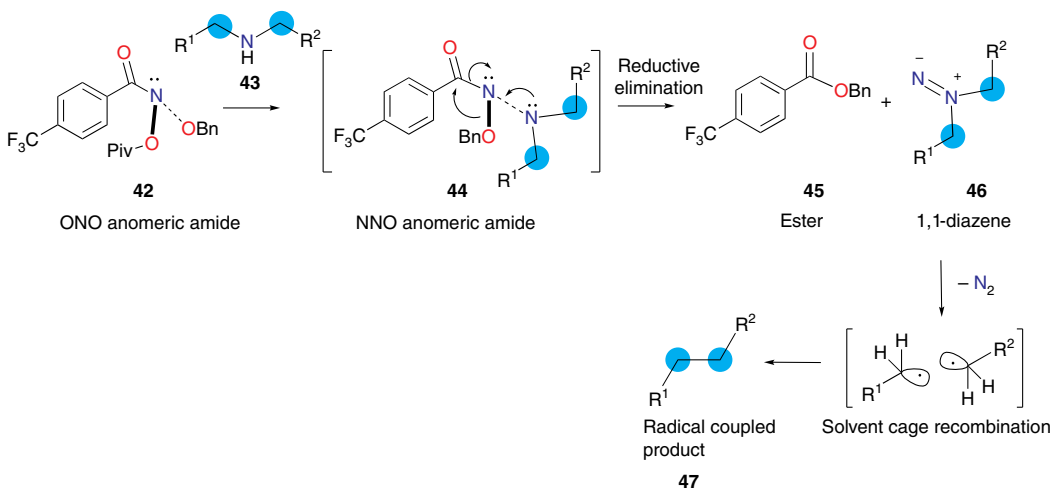

Scheme 4. Editing nitrogen from secondary amines using an *N*-acyloxy-*N*-alkoxyamide **42**.

Correcting the initial activity of **42** yields an activity of LogTA100 = 2.6 (Fig. 14) and **42** would generate between 270 and 580 induced revertants at 1 µmol per plate. The QSAR points to **42** being at least as mutagenic as our standard, *N*-acetoxy-*N*-butoxybenzamide (**9**, X = H), which we have reproduced many times in the Ames studies.

Levin used other NAAs, **48**, **49a–c**, **50** and **51** (Chart 13), in the development of reagent **42**. **48** is a proven mutagen; in an early study, we reported its activity at 1 µmol per plate to be LogTA100 = 2.63.[40] After steric correction for the pivaloyloxyl group, **49a–c** and **50** are predicted to have very similar activity to that of **42** and **48** (Table 10) with activity of **51** slightly lower.

Of the wide range of some 100 NAAs for which we have mutagenicity data, which accounts for almost all known NAAs, only three, **15d**, **16b** and **17d**, failed to generate a dose response in TA100 and can be considered to be non-mutagenic, while **15a** and **15b** generated very shallow dose responses and are weakly mutagenic according to the protocols (LogTA100 < 2).[41,59] As outlined in 'Steric effects on activity', non-mutagenicity of **15d** and **16b** has been attributed to their inability to enter the major groove of DNA on account of their overall dimensions.[52,59] The negative result for **17d** in the Ames test was in accord with its resistance to S_N2 reaction with *N*-methylaniline.[59] It is possible that **15d** or **16b** may be suitable candidates for nitrogen deletion from amines in spectral editing.

The QSAR we have developed would strongly suggest that **42** will be a *direct-acting* mutagen and must be handled very carefully by practitioners in the field. It is important that **42**, or any analogues thereof, should not be declared to be safe reagents for wide use in skeletal editing, and for synthesis in large quantities for routine use, until it is proved not to produce

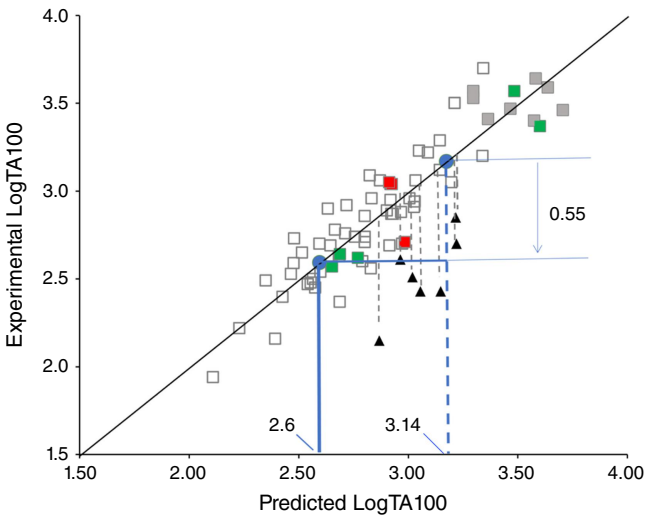

Fig. 14. Predicted vs experimental activities of mutagenic *N*-acyloxy-*N*-alkoxyamides, at 1 µmol per plate; training set, filled and open squares (new data: fluorene in red, fluorenones in green); **18a–g**, filled triangles; **42**, filled circles.

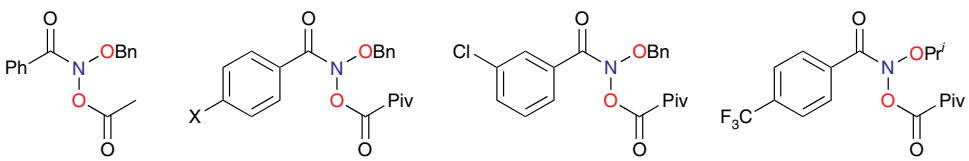

Chart 13. NAAs used in development of skeletal-editing agent **42**.

Table 10. Relevant QSAR parameters and predicted LogTA100 of *N*-acyloxy-*N*-alkoxyamides **42**, **49a–c**, **50** and **51** using the QSAR in Eqn 10.

Structure	Log *P*	pK_a	E_s[A]	LogTA100		Pred.[D]
				Pred.[B]	Adjusted[C]	
42	5.78	5.03	−2.40	3.14	2.59	393
49a	4.86	5.03	0	3.17	2.62	419
49b	5.35	5.03	−1.24	3.16	2.61	409
49c	4.73	5.03	−0.55	3.08	2.53	342
50	5.42	5.03	0	3.31	2.76	570
51	4.70	5.03	−2.40	2.88	2.33	215

[A]Taft steric parameters for *para*-benzamide substituents.
[B]Calculated from Eqn 10.
[C]Calculated LogTA100 − 0.55.
[D]Predicted revertants at adjusted LogTA100.

a dose response in the Ames reverse mutation test. It is incumbent on the author to inform users of Levin's skeletal editing method, those employing other NAAs for variations thereof or for other means, of the mutagenic properties of almost all known variants. Eqns 6, 7, 10 provide useful means of predicting *a priori* the likelihood and extent of mutagenic activity.

Conclusion

N-Acyloxy-*N*-alkoxyamides, as a class of anomeric amides, are mutagenic in the Ames reverse mutation assay with point mutation strain TA100, and select members bearing intercalating groups are active in frameshift strain TA98, in both cases without the need for metabolic activation. They have been shown to react with plasmid DNA, primarily at N7 of guanine in the major groove of DNA. As such, their mutagenic activity can be used to determine the factors controlling ease of access to bacterial DNA, binding modes with DNA and the ease of reaction with the guanosine nucleoside in the bound state. The Ames test requires minimal quantities of these compounds, which are easily synthesised in small amounts with a high degree of structural diversity. Almost all are heavy oils, which can be safely procured, purified, characterised and tested without exposure.

By measuring and comparing the mutagenicity at 1 μmol per plate with TA100 in a standardised manner, we have been able to establish how their activity is related to their structural features. For comparisons with our data, any new compound should be tested with the standard (9, X = H), which serves both as a cross-check of the test system as well as a means of relating activities. Quantitative structure–activity relationships have been established enabling identification of trends and processes of importance to small molecule–DNA interactions. We have developed QSARS catering for hydrophobic properties of the molecules, chemical reactivity at the electrophilic nitrogen, steric effects on all three side chains and intercalative ability of planar polycyclic aromatics. Based on the mutagenic activity of many structural and regioisomers, the QSARs are accurate to the point of identifying impacts of small structural changes on ease of groove binding or of intercalation. They can also be used to focus on bacterial metabolic processes and mechanisms of DNA damage and to identify substructure potentially deleterious to DNA binding and reaction with DNA, as well as to predict, in advance, the mutagenic properties of new congeners.

All this is made possible on account of their anomeric substitution at nitrogen with both a donor alkoxyl and an acceptor acyloxyl group. The electronegativity of oxygen atoms at nitrogen results in greatly reduced amide resonance and nitrogens that are quite atypical of those in more common primary, *N*-alkyl secondary and *N*,*N*-dialkyl tertiary amides. Their pyramidality, combined with the anomeric interaction between the nitrogen substituents, both properties of which we have developed a thorough understanding, are entirely responsible for their reaction, directly, with nucleophilic sites in DNA.

Note in proof

The skeletal editing agent **42** has recently been shown to be a direct-acting mutagen in the Ames II assay.[108] Qualitative results from the Ames II method, which detects point mutations in a mix of *S. typhimurium* strains, are generally in good agreement with those from the full plate Ames methodology using TA100.[109] Contrary to Levin's recently published view,[108] quantitative Ames II results for **42** with *S. typhimurium* TA7001-7006 cannot be compared meaningfully to predicted plate counts from the standard Ames test with *S. typhimurium* TA100.

Supplementary material

Supplementary material is available online.

References

[1] Glover SA. Anomeric Amides — Structure, Properties and Reactivity. *Tetrahedron* 1998; 54: 7229–7271. doi:10.1016/S0040-4020(98)00197-5

[2] Alabugin IV, Bresch S, Manoharan M. Hybridization Trends for Main Group Elements and Expanding the Bent's Rule Beyond Carbon: More than Electronegativity. *J Phys Chem A* 2014; 118: 3663–3677. doi:10.1021/jp502472u

[3] Bent HA. An Appraisal of Valence-bond Structures and Hybridization in Compounds of the First-row Elements. *Chem Rev* 1961; 61: 275–311. doi:10.1021/cr60211a005

[4] Rauk A, Glover SA. A Computational Investigation of the Stereoisomerism in Heteroatom-substituted Amides. *J Org Chem* 1996; 61: 2337–2345. doi:10.1021/jo9521817

[5] Glover SA, Rauk A. Conformational Stereochemistry of the HERON Amide, *N*-methoxy-*N*-dimethylaminoformamide: a Theoretical Study. *J Org Chem* 1999; 64: 2340–2345. doi:10.1021/jo982048p

[6] Glover SA, Mo G, Rauk A, Tucker DJ, Turner P. Structure, conformation, anomeric effects and rotational barriers in the HERON amides, *N*,*N*'-diacyl-*N*,*N*'-dialkoxyhydrazines. *J Chem Soc, Perkin Trans 2* 1999; 2053–2058. doi:10.1039/a904575i

[7] Gillson A-ME, Glover SA, Tucker DJ, Turner P. Crystal structures and properties of mutagenic *N*-acyloxy-*N*-alkoxyamides — 'most pyramidal' acyclic amides. *Org Biomol Chem* 2003; 1: 3430–3437. doi:10.1039/B306098P

[8] Glover SA. *N*-Acyloxy-*N*-alkoxyamide – Structure, properties, reactivity and biological activity. In Richard J, editor. Advances in Physical Organic Chemistry. Vol. 42. London: Elsevier; 2008. pp. 35–123.

[9] Glover SA. *N*-Heteroatom-substituted hydroxamic esters. In Rappoport Z, Liebman JF, editors. The Chemistry of Hydroxylamines, Oximes and Hydroxamic, Acids, Part 2. Chichester: Wiley; 2009. pp. 839–923.

[10] Glover SA, White JM, Rosser AA, Digianantonio KM. Structures of *N*,*N*-Dialkoxyamides: Pyramidal Anomeric Amides with Low Amidicity. *J Org Chem* 2011; 76: 9757–9763. doi:10.1021/jo201856u

[11] Glover SA, Rosser AA, Taherpour A, Greatrex BW. Formation and HERON Reactivity of Cyclic *N,N*-Dialkoxyamides. *Aust J Chem* 2014; 67: 507–520. doi:10.1071/CH13557
[12] Glover SA, Rosser AA, Spence RM. Studies of the Structure, Amidicity and Reactivity of *N*-Chlorohydroxamic Esters and *N*-Chloro-β,β-dialkylhydrazides: Anomeric Amides with Low Resonance Energies. *Aust J Chem* 2014; 67: 1344–1352. doi:10.1071/CH14270
[13] Glover SA, Rosser AA. Heteroatom Substitution at Amide Nitrogen – Resonance Reduction and HERON Reactions of Anomeric Amides. *Molecules* 2018; 23: 2834. doi:10.3390/molecules23112834
[14] Bonin AM, Glover SA, Hammond GP. Reactive intermediates from the solvolysis of mutagenic *O*-alkyl *N*-acetoxybenzohydroxamates. *J Chem Soc, Perkin Trans 2* 1994; 1173–1180. doi:10.1039/p29940001173
[15] Campbell JJ, Glover SA, Hammond GP, Rowbottom CA. Evidence for the Formation of Nitrenium ions in the Acid-catalysed Solvolysis of Mutagenic *N*-acetoxy-*N*-Alkoxybenzamides. *J Chem Soc, Perkin Trans 2* 1991; 2067–2079. doi:10.1039/p29910002067
[16] Cavanagh KL, Glover SA, Price HL, Schumacher RR. S_N2 Substitution Reactions at the Amide Nitrogen in the Anomeric Mutagens, *N*-Acyloxy-*N*-alkoxyamides. *Aust J Chem* 2009; 62: 700–710. doi:10.1071/CH09166
[17] Glover SA. S_N2 reactions at amide nitrogen – theoretical models for reactions of mutagenic *N*-acyloxy-*N*-alkoxyamides with bio-nucleophiles (OT-308CP). *Arkivoc* 2001; (xii): 143–160. doi:10.3998/ark.5550190.0002.c15
[18] Campbell JJ, Glover SA. Bimolecular Reactions of Mutagenic *N*-(Acyloxy)-*N*-alkoxybenzamides with Aromatic Amines. *J Chem Res (S)*. 1999; 23: 474–475. doi:10.1177/174751989902300810
[19] Campbell JJ, Glover SA. Bimolecular Reactions of Mutagenic *N*-(Acyloxy)-*N*-alkoxybenzamides with Aromatic Amines. *J Chem Res (M)*. 1999; 23: 2075–2096.
[20] Campbell JJ, Glover SA. Bimolecular Reactions of Mutagenic *N*-Acetoxy-*N*-alkoxybenzamides and *N*-methylaniline. *J Chem Soc, Perkin Trans 2* 1992; 1661–1663. doi:10.1039/p29920001661
[21] Glover SA, Mo G. Hindered ester formation by S_N2 azidation of *N*-acetoxy-*N*-alkoxyamides and *N*-alkoxy-*N*-chloroamides—Novel application of HERON rearrangements. *J Chem Soc, Perkin Trans 2* 2002; 1728–1739. doi:10.1039/B111250N
[22] Glover SA, Hammond GP, Bonin AM. A Comparison of the Reactivity and Mutagenicity of *N*-(Benzoyloxy)-*N*-(benzyloxy) benzamides. *J Org Chem* 1998; 63: 9684–9689. doi:10.1021/jo980863z
[23] Glover SA, Adams M. Reaction of *N*-acyloxy-*N*-alkoxyamides with Biological Thiol groups. *Aust J Chem* 2011; 64: 443–453. doi:10.1071/CH10470
[24] Johns JP, van Losenoord A, Mary C, Garcia P, Pankhurst DS, Rosser AA, Glover SA. Thermal Decomposition of *N*-Acyloxy-*N*-alkoxyamides – a New HERON Reaction. *Aust J Chem* 2010; 63: 1717–1729. doi:10.1071/CH10350
[25] Beland FA, Kadlubar FF. Metabolic activation and DNA adducts of aromatic amines and nitroaromatic hydrocarbons. In Cooper CS, Grover PL, editors. Chemical Carcinogenesis and Mutagenesis, 8 edn. Secaucus, NJ: Springer Verlag; 1990. pp. 267–325.
[26] Beland FA, Kadlubar FF. Formation and Persistence of Arylamine DNA Adducts in Vivo. *Environ Health Perspect* 1985; 62: 19–30. doi:10.1289/ehp.856219
[27] Blackburn GM, Kellard B. Chemical carcinogens - II. *Chem Ind* 1986; 687–695.
[28] Kim D, Guengerich FP. Cytochrome P450 Activation of Arylamines and Heterocyclic Amines. *Annu Rev Pharmacol Toxicol* 2005; 45: 27–49. doi:10.1146/annurev.pharmtox.45.120403.100010
[29] Miller JA, Miller EC. Some Historical Aspects of *N*-Aryl Carcinogens and Their Metabolic Activation. *Environ Health Perspect* 1983; 49: 3–12. doi:10.1289/ehp.83493
[30] Novak M, Rajagopal S. N-arylnitrenium ions. *Adv Phys Org Chem* 2001; 36: 167–254. doi:10.1016/S0065-3160(01)36005-7
[31] Novak M, Rajagopal S. Correlations of Nitrenium Ion Selectivities with Quantitative Mutagenicity and Carcinogenicity of the Corresponding Amines. *Chem Res Toxicol* 2002; 15: 1495–1503. doi:10.1021/tx025584s
[32] Novak M, Kahley MJ, Eiger E, Helmick JS, Peters HE. Reactivity and Selectivity Of Nitrenium Ions Derived from Ester Derivatives of Carcinogenic *N*-(4-Biphenylyl)hydroxylamine and the Corresponding Hydroxamic Acid. *J Am Chem Soc* 1993; 115: 9453–9460. doi:10.1021/ja00074a010
[33] Davidse PA, Kahley MJ, McClelland RA, Novak M. Flash Photolysis Observation and Lifetimes of 2-Fluorenyl- and 4-Biphenylylacetylnitrenium Ions in Aqueous Solution. *J Am Chem Soc* 1994; 116: 4513–4514. doi:10.1021/ja00089a065
[34] Gerdes RG, Glover SA, Ten Have JF, Rowbottom CA. *N*-Acetoxy-*N*-alkoxyamides - a new class of nitrenium ion precursors, which are mutagenic. *Tetrahedron Lett* 1989; 30: 2649–2652. doi:10.1016/S0040-4039(00)99089-0
[35] Campbell JJ, Glover SA, Rowbottom CA. Solvolysis and Mutagenesis of *N*-Acetoxy-*N*-Alkoxybenzamides — Evidence for Nitrenium Ion Formation. *Tetrahedron Lett* 1990; 31: 5377–5380. doi:10.1016/S0040-4039(00)98076-6
[36] Glover SA, Scott AP. MNDO properties of heteroatom and phenyl-substituted nitrenium ions. *Tetrahedron* 1989; 45: 1763–1776. doi:10.1016/S0040-4020(01)80041-7
[37] Glover SA, Goosen A, McCleland CW, Schoonraad JL. *N*-Alkoxy-*N*-acylnitrenium Ions as Possible Intermediates in Intramolecular Aromatic Substitution: Novel Formation of *N*-Acyl-3,4-dihydro-1*H*-2,1-benzoxazines and *N*-Acyl-4,5-dihydro-1*H*,3*H*-2,1-benzoxazepine. *J Chem Soc, Perkin Trans 1* 1984; 2255–2260. doi:10.1039/p19840002255
[38] Banks TM, Bonin AM, Glover SA, Prakash AS. Mutagenicity and DNA Damage Studies of *N*-acyloxy-*N*-alkoxyamides — the Role of Electrophilic Nitrogen. *Org Biomol Chem* 2003; 1: 2238–2246. doi:10.1039/b301618h
[39] Banks TM. Reactivity, Mutagenicity and DNA damage of *N*-Acyloxy-*N*-alkoxyamides. PhD thesis, University of New England, Armidale; 2003.
[40] Bonin AM, Banks TM, Campbell JJ, Glover SA, Hammond GP, Prakash AS, Rowbottom CA. Mutagenicity of Electrophilic *N*-acyloxy-*N*-alkoxyamides. *Mutat Res Genet Toxicol Environ Mutagen* 2001; 494: 115–134. doi:10.1016/S1383-5718(01)00189-9
[41] Mortelmans K, Zeiger E. The Ames *Salmonella*/microsome mutagenicity assay. *Mutat Res Fundam Mol Mech Mutagen* 2000; 455: 29–60. doi:10.1016/S0027-5107(00)00064-6
[42] Banks TM, Clay SF, Glover SA, Schumacher RR. Mutagenicity of *N*-acyloxy-*N*-alkoxyamides as an indicator of DNA intercalation Part 1: Evidence for naphthalene as a DNA intercalator. *Org Biomol Chem* 2016; 14: 3699–3714. doi:10.1039/C6OB00162A
[43] Hansch C, Leo AJ. Exploring QSAR, Fundamentals and Applications in Chemistry and Biology, Part I. Washington DC: American Chemical Society; 1995.
[44] Debnath AK, Shusterman AJ, Lopez de Compadre RL, Hansch C. The importance of the hydrophobic interaction in the mutagenicity of organic compounds. *Mutat Res Fundam Mol Mech Mutagen* 1994; 305: 63–72. doi:10.1016/0027-5107(94)90126-0
[45] Debnath AK, Hansch C. The importance of hydrophobicity in the mutagenicity of methanesulfonic acid esters with salmonella typhimurium TA100. *Chem Res Toxicol* 1993; 6: 310–312. doi:10.1021/tx00033a009
[46] Debnath AK, Lopez de Compadre RL, Debnath G, Shusterman AJ, Hansch C. Structure–activity relationship of mutagenic aromatic and heteroaromatic nitro compounds. Correlation with molecular orbital energies and hydrophobicity. *J Med Chem* 1991; 34: 786–797. doi:10.1021/jm00106a046
[47] De Compadre RLL, Shusterman AJ, Hansch C. The Role of Hydrophobicity in the Ames Test. The Correlation of the Mutagenicity of Nitropolycyclic Hydrocarbons with Partition Coefficients and Molecular Orbital Indices. *Int J Quantum Chem* 1988; 34: 91–101. doi:10.1002/qua.560340202
[48] Leo AJ, Hansch C. Role of hydrophobic effects in mechanistic QSAR. *Perspect Drug Discovery Des* 1999; 17: 1–25. doi:10.1023/A:1008762321231
[49] Ghose AK, Pritchett A, Crippen GM. Atomic Physicochemical Parameters for Three-Dimensional Structure Directed

Quantitative Structure–Activity Relationships III: Modeling Hydrophobic Interactions. *J Comput Chem* 1988; 9: 80–90. doi:10.1002/jcc.540090111
[50] Andrews LE, Banks TM, Bonin AM, Clay SF, Gillson A-ME, Glover SA. Mutagenic *N*-acyloxy-*N*-alkoxyamides: Probes for Drug–DNA Interactions. *Aust J Chem* 2004; 57: 377–381. doi:10.1071/CH03276
[51] Hansch C, Leo AJ, Hoekman D. Exploring QSAR, Fundamentals and Applications in Chemistry and Biology, Part II. Washington, DC: American Chemical Society; 1995.
[52] Glover SA, Schumacher RR. The effect of hydrophobicity upon the direct mutagenicity of *N*-acyloxy-*N*-alkoxyamides – Bilinear dependence upon Log*P*. *Mutat Res Genet Toxicol Environ Mutagen* 2016; 795: 41–50. doi:10.1016/j.mrgentox.2015.11.005
[53] Tuppurainen K. Frontier orbital energies, hydrophobicity and steric factors as physical QSAR descriptors of molecular mutagenicity. A review with a case study: MX compounds. *Chemosphere* 1999; 38: 3015–3030. doi:10.1016/S0045-6535(98)00503-7
[54] Ames BN, Lee FD, Durston WE. An Improved Bacterial Test System for the Detection and Classification of Mutagens and Carcinogens. *Proc Natl Acad Sci U S A* 1973; 70: 782–786. doi:10.1073/pnas.70.3.782
[55] Lipinski CA, Lombardo F, Dominy BW, Feeney PJ. Experimental and computational approaches to estimate solubility and permeability in drug discovery and development settings. *Adv Drug Delivery Rev* 2001; 46: 3–26. doi:10.1016/S0169-409X(00)00129-0
[56] Kubinyi H. Quantitative structure–activity relations. 7. The bilinear model, a new model for non-linear dependence of biological activity on hydrophobic character. *J Med Chem* 1977; 20: 625–629. doi:10.1021/jm00215a002
[57] Kubinyi H. Lipophilicity and drug activity. In Jucker E, editor. Progress in Drug Research. Vol. 23. Birkhäuser Basel; 1979. pp. 97–198. doi:10.1007/978-3-0348-7105-1_5
[58] Kubinyi H, Kehrhahn OH. Quantitative Structure–Activity relationships. VI. Non-linear dependence of biological activity on hydrophobic character: Calculation procedures for bilinear model. *Arzneimittel-Forschung* 1978; 28: 598–601.
[59] Andrews LE, Bonin AM, Fransson LE, Gillson A-ME, Glover SA. The Role of Steric Effects in the Direct Mutagenicity of *N*-Acyloxy-*N*-alkoxyamides. *Mutat Res Genet Toxicol Environ Mutagen* 2006; 605: 51–62. doi:10.1016/j.mrgentox.2006.02.003
[60] De Kimpe N, Verhé R. Synthesis and reactivity of α-halogenated ketones. In Patai S, Rappoport Z, editors. α-Haloketones, α-Haloaldehydes and α-Haloimines. John Wiley & Sons, Inc; 1988. pp. 1–119.
[61] Glover SA, Schumacher RR, Bonin AM, Fransson LE. Steric effects on the direct mutagenicity of *N*-acyloxy-*N*-alkoxyamides – probes for drug–DNA interactions. *Mutat Res Genet Toxicol Environ Mutagen* 2011; 722: 32–38. doi:10.1016/j.mrgentox.2011.02.007
[62] Neidle S. Principles of Small Molecule-DNA Recognition. New York: Academic Press; 2008. pp. 132–203.
[63] Blackburn GM, Gait MJ, Loakes D, Williams DM. Nucleic Acids in Chemistry and Biology. Cambridge: RSC Publishing; 2006.
[64] Graves DE, Velea LM. Intercalative Binding of Small Molecules to Nucleic Acids. *Curr Org Chem* 2000; 4: 915–929. doi:10.2174/1385272003375978
[65] Pindur U, Haber M, Sattler K. Antitumor Active Drugs as Intercalators of Deoxyribonucleic Acid. *J Chem Educ* 1993; 70: 263–272. doi:10.1021/ed070p263
[66] Qian X, Huang T-B, Wei D-z, Zhu D-H, Zhu , Yao W. Interaction of naphthyl heterocycles with DNA: effects of thiono and thio groups. *J Chem Soc, Perkin Trans 2* 2000; 715–718. doi:10.1039/a908787g
[67] Sartorius J, Schneider H-J. Intercalation mechanisms with ds-DNA: binding modes and energy contributions with benzene, naphthalene, quinoline and indole derivatives including some antimalarials. *J Chem Soc, Perkin Trans 2* 1997; 2319–2328. doi:10.1039/a702628e
[68] Stevenson KA, Yen SF, Yang NC, Boykin DW, Wilson WD. A substituent constant analysis of the interaction of substituted naphthalene monoimides with DNA. *J Med Chem* 1984; 27: 1677–1682. doi:10.1021/jm00378a026
[69] Chu Y, Hoffman DW, Iverson BL. A Pseudocatenane Structure Formed between DNA and a Cyclic Bisintercalator. *J Am Chem Soc* 2009; 131: 3499–3508. doi:10.1021/ja805676w
[70] Yen SF, Gabbay EJ, Wilson WD. Interaction of aromatic imides with DNA. 1. Spectrophotometric and viscometric studies. *Biochemistry* 1982; 21: 2070–2076. doi:10.1021/bi00538a014
[71] Wilson WD. Comprehensive Natural Product Chemistry. Oxford: Pergamon; 1999. pp. 427–476.
[72] Chaires JB. Energetics of drug-DNA interactions. *Biopolymers* 1997; 44: 201–215. doi:10.1002/(SICI)1097-0282(1997)44:3<201::AID-BIP2>3.0.CO;2-Z
[73] Lerman LS. The Structure of the DNA–Acridine Complex. *Proc Natl Acad Sci U S A* 1963; 49: 94–102. doi:10.1073/pnas.49.1.94
[74] Lerman LS. Structural considerations in the interaction of DNA and acridines. *J Mol Biol* 1961; 3: 18–30. doi:10.1016/S0022-2836(61)80004-1
[75] Neidle S. Nucleic Acid Structure and Recognition. Oxford: Oxford University Press; 2002.
[76] Ames BN, Gurney EG, Miller JA, Bartsch H. Carcinogens as Frameshift Mutagens: Metabolites and Derivatives of 2-Acetylaminofluorene and Other Aromatic Amine Carcinogens. *Proc Natl Acad Sci U S A* 1972; 69: 3128–3132. doi:10.1073/pnas.69.11.3128
[77] Isono K, Yourno J. Chemical Carcinogens as Frameshift Mutagens: *Salmonella* DNA Sequence Sensitive to Mutagenesis by Polycyclic Carcinogens. *Proc Natl Acad Sci U S A* 1974; 71: 1612–1617. doi:10.1073/pnas.71.5.1612
[78] Ames BN, Durston WE, Yamasaki E, Lee FD. Carcinogens are Mutagens: A Simple Test System Combining Liver Homogenates for Activation and Bacteria for Detection. *Proc Natl Acad Sci U S A* 1973; 70: 2281–2285. doi:10.1073/pnas.70.8.2281
[79] Creech HJ, Preston RK, Peck RM, O'Connell AP, Ames BN. Antitumor and mutagenic properties of a variety of heterocyclic nitrogen and sulfur mustards. *J Med Chem* 1972; 15: 739–746. doi:10.1021/jm00277a011
[80] Glover SA, Schumacher RR. Mutagenicity of *N*-acyloxy-*N*-alkoxyamides as an indicator of DNA intercalation: The role of fluorene and fluorenone substituents as DNA intercalators. *Mutat Res Genet Toxicol Environ Mutagen* 2021; 863–864: 503299. doi:10.1016/j.mrgentox.2020.503299
[81] Schumacher RR. Structural Effects upon the Mutagenicity of *N*-acyloxy-*N*-alkoxyamides. PhD thesis, University of New England, Armidale; 2011.
[82] Zegar IS, Prakash AS, Harvey RG, LeBreton PR. Stereoelectronic aspects of the intercalative binding properties of 7, 12-dimethylbenz[*a*]anthracene metabolites with DNA. *J Am Chem Soc* 1985; 107: 7990–7995. doi:10.1021/ja00312a033
[83] Zang H, Gates KS. DNA Binding and Alkylation by the 'Left Half' of Azinomycin B. *Biochemistry* 2000; 39: 14968–14975. doi:10.1021/bi001998d
[84] Alcaro S, Coleman RS. A Molecular Model for DNA Cross-Linking by the Antitumor Agent Azinomycin B. *J Med Chem* 2000; 43: 2783–2788. doi:10.1021/jm990362l
[85] Alcaro S, Ortuso F, Coleman RS. DNA Cross-Linking by Azinomycin B: Monte Carlo Simulations in the Evaluation of Sequence Selectivity. *J Med Chem* 2002; 45: 861–870. doi:10.1021/jm011040w
[86] Coleman RS, Perez RJ, Burk CH, Navarro A. Studies on the Mechanism of Action of Azinomycin B: Definition of Regioselectivity and Sequence Selectivity of DNA Cross-Link Formation and Clarification of the Role of the Naphthoate. *J Am Chem Soc* 2002; 124: 13008–13017. doi:10.1021/ja025563k
[87] Coleman RS, Tierney MT, Cortright SB, Carper DJ. Synthesis of Functional 'Top-Half' Partial Structures of Azinomycin A and B. *J Org Chem* 2007; 72: 7726–7735. doi:10.1021/jo7014888
[88] Casely-Hayford MA, Pors K, James CH, Patterson LH, Hartley JA, Searcey M. Design and synthesis of a DNA-crosslinking azinomycin analogue. *Org Biomol Chem* 2005; 3: 3585–3589. doi:10.1039/b508908e

[89] Bair KW, Tuttle RL, Knick VC, Cory M, McKee DD. [(1-Pyrenylmethyl)amino]alcohols, a new class of antitumor DNA intercalators. Discovery and initial amine side chain structure–activity studies. *J Med Chem* 1990; 33: 2385–2393. doi:10.1021/jm00171a012
[90] Secco F, Venturini M, Biver T, Sánchez F, Prado-Gotor R, Grueso E. Solvent Effects on the Kinetics of the Interaction of 1-Pyrenecarboxaldehyde with Calf Thymus DNA. *J Phys Chem B* 2010; 114: 4686–4691. doi:10.1021/jp910411c
[91] Laib S, Krieg A, Häfliger P, Agorastos N. DNA-intercalation on pyrene modified surface coatings. *Chem Commun* 2005; 5566–5568. doi:10.1039/b511716j
[92] Nakamura M, Fukunaga Y, Sasa K, Ohtoshi Y, Kanaori K, Hayashi H, Nakano H, Yamana K. Pyrene is highly emissive when attached to the RNA duplex but not to the DNA duplex: the structural basis of this difference. *Nucleic Acids Res* 2005; 33: 5887–5895. doi:10.1093/nar/gki889
[93] Förster U, Grünewald C, Engels JW, Wachtveitl J. Ultrafast Dynamics of 1-Ethynylpyrene-Modified RNA: A Photophysical Probe of Intercalation. *J Phys Chem B* 2010; 114: 11638–11645. doi:10.1021/jp103176q
[94] Chen F-M. Binding of pyrene to DNA, base squence specificity and its implication. *Nucleic Acids Res* 1983; 11: 7231–7250. doi:10.1093/nar/11.20.7231
[95] Becker H-C, Nordén B. DNA Binding Mode and Sequence Specificity of Piperazinylcarbonyloxyethyl Derivatives of Anthracene and Pyrene. *J Am Chem Soc* 1999; 121: 11947–11952. doi:10.1021/ja991844p
[96] Jiang Z, Zhang Y, Yu Y, Wang Z, Zhang X, Duan X, Wang S. Study on Intercalations between Double-Stranded DNA and Pyrene by Single-Molecule Force Spectroscopy: Toward the Detection of Mismatch in DNA. *Langmuir* 2010; 26: 13773–13777. doi:10.1021/la102647p
[97] Debnath AK, Lopez Compadre RL, Shusterman AJ, Hansch C. Quantitative Structure–Activity Relationship Investigation of the Role of Hydrophobicity in Regulating Mutagenicity in the Ames Test: 2. Mutagenicity of Aromatic and Heteroaromatic Nitro Compounds in *Salmonella typhimurium* TA100. *Env Mol Mutagen* 1992; 19: 53–70. doi:10.1002/em.2850190108
[98] Klein M, Voigtmann U, Haack T, Erdinger L, Boche G. From mutagenic to non-mutagenic nitroarenes: effect of bulky alkyl substituents on the mutagenic activity of 4-nitrobiphenyl in *Salmonella typhimurium*: Part I. Substituents ortho to the nitro group and in 2′-position. *Mutat Res Genet Toxicol Environ Mutagen* 2000; 467: 55–68. doi:10.1016/S1383-5718(00)00012-7
[99] Klein M, Erdinger L, Boche G. From mutagenic to non-mutagenic nitroarenes: effect of bulky alkyl substituents on the mutagenic activity of nitroaromatics in *Salmonella typhimurium*: Part II. Substituents far away from the nitro group. *Mutat Res Genet Toxicol Environ Mutagen* 2000; 467: 69–82. doi:10.1016/S1383-5718(00)00013-9
[100] Kennedy SH, Dherange BD, Berger KJ, Levin MD. Skeletal editing through direct nitrogen deletion of secondary amines. *Nature* 2021; 593: 223–227. doi:10.1038/s41586-021-03448-9
[101] Berger KJ, Driscoll JL, Yuan M, Dherange BD, Gutierrez O, Levin MD. Direct Deamination of Primary Amines via Isodiazene Intermediates. *J Am Chem Soc* 2021; 143: 17366–17373. doi:10.1021/jacs.1c09779
[102] Glover SA, Rauk A, Buccigross JM, Campbell JJ, Hammond GP, Mo G, Andrews LE, Gillson A-ME. The HERON reaction – Origin, Theoretical Background, and Prevalence. *Can J Chem* 2005; 83: 1492–1509. doi:10.1139/v05-150
[103] Glover SA, Mo G, Rauk A. HERON rearrangement of *N,N*'-diacyl-*N,N*'-dialkoxyhydrazines – a theoretical and experimental study. *Tetrahedron* 1999; 55: 3413–3426. doi:10.1016/S0040-4020(98)01151-X
[104] Buccigross JM, Glover SA. Molecular orbital studies of novel N to C migrations in *N,N*-bisheteroatom-substituted amides—HERON rearrangements. *J Chem Soc, Perkin Trans 2* 1995; 595–603. doi:10.1039/P29950000595
[105] Glover SA. HERON Rearrangement (Heteroatom Rearrangements on Nitrogen). In O'Neil MJ, editor. Merck Index, Organic Name Reactions ONR-48, 13 edn. Whitehouse Station, N.J.: Merck & Co., Inc.; 2001.
[106] Unsworth WP, Avestro A-J. Nitrogen deletion offers fresh strategy for organic synthesis. *Nature* 2021; 593: 203–204. doi:10.1038/d41586-021-01205-6
[107] Zippel C, Seibert J, Bräse S. Skeletal Editing—Nitrogen Deletion of Secondary Amines by Anomeric Amide Reagents. *Angew Chem Int Ed* 2021; 60: 19522–19524. doi:10.1002/anie.202107490
[108] Dherange BD, Yuan M, Kelly CB, Reiher CA, Grosanu C, Berger KJ, Gutierrez O, Levin MD. Direct deaminative functionalization. *J Am Chem Soc* 2023; 145: 17–24. https://doi.org/10.1021/jacs.2c11453, S2 of Supporting Information
[109] Kamber M, Flückiger-Isler S, Engelhardt G, Jaeckh R and Zeiger E. Comparison of the Ames II and traditional Ames test responses with respect to mutagenicity, strain specificities, need for metabolism and correlation with rodent carcinogenicity. *Mutagenesis* 2009; 24: 359–366. https://doi.org/10.1093/mutage/gep017

Data availability. The data used in this account are supplied as Electronic Supplementary Material.

Conflicts of interest. The author declares no conflict of interest.

Declaration of funding. This work did not receive any specific funding.

Acknowledgements. The author is indebted to the many students whose work is cited in this Account, as well as to Dr Tony Bonin who contributed his valuable expertise to early Ames testing of our compounds and to the establishment of the testing facility at UNE.

Author affiliation
[A]Department of Chemistry, School of Physical Sciences, University of New England, NSW 2350, Australia.